A DISSERTATION

ON

Solar Photovoltaic String Under Partial Condition With Irradiance

Submitted In Partial Fulfilment of the Requirement for the Award of the Degree in

M.Tech

In

Electronic Circuits and Systems

Submitted By

Anjali Verma

Roll No.: 2101311001

Under the Guidance of

Mr. Mohd Javed Khan
(Supervisor)

Mr. Saif Ahmad
(Co-Supervisor)

Department of Electronics & Communication Engineering,

Integral University, Lucknow-226026

June-2023

DECLARATION

This is to certify that I, Anjali Verma,(Roll No.: 2101311001) have completed the M.Tech Dissertation work on topic **"Solar Photovoltaic String under partial condition with irradiance"** under the supervision of Mr. Mohd Javed Khan and Mr. Saif Ahmad for the partial fulfillment of the requirement for the Master of Technology in Electronics Circuits and systems from Department of Electronics and Communication Engineering, Integral University, Lucknow. This is an original piece of work & I have not submitted it earlier elsewhere.

Date:

Place:

Signatuure

Anjali Verma

Roll No.: 2101311001

CERTIFICATE

This is to certify that the dissertation titled **"Solar Photovoltaic String under partial condition with irradiance"** has been carried out by Anjali Verma(Roll No.: 2101311001) under my supervision and guidance in partial fulfilment of the requirements for the award of degree of "Master of Technology" in Electronic Circuits and Systems at department of Electronics and Communication Engineering, Integral University, Lucknow, India.

Mr. Mohd Javed Khan
Supervisor
Assistant Professor
Dept. of ECE,
Integral University,
Lucknow

Mr. Saif Ahmad
Co-Supervisor
Assistant Professor
Dept. of ECE,
Integral University,
Lucknow

ACKNOWLEDGEMENT

I wish to express my sincere thanks to my supervisor, Mr. Mohd Javed Khan, Assistant Professor, Department of Electronics & Communication Engineering, and Co-supervisor, Mr. Saif Ahmad, Assistant Professor, Department of Electronics & Communication Engineering whose sincerity and encouragement I will never forget. This work would not have been possible without the support and valuable guidance of my supervisor and co-supervisor.

I sincerely wish to thank, Prof. Syed Hasan Saeed, Professor (HOD, Department of Electronics & Communication Engineering) for his valuable feedbacks during my comprehensive examination. I also thankful to all the faculty members and my colleagues who helped me in any way in completion of this dissertation.

Last but not the least, I would like to thanks and my family and friends for supporting me throughout writing this dissertation.

Anjali Verma

Roll No.: 2101311001

ABSTRACT

A photovoltaic system is highly susceptible to partial shading. Based on the functionality of a photovoltaic system that relies on solar irradiance to generate electrical power, it is tacitly assumed that the maximum power of a partially shaded photovoltaic system always decreases as the shading heaviness increases. However, the literature has reported that this might not be the case. The maximum power of a partially shaded photovoltaic system under a fixed configuration and
partial shading pattern can be highly insusceptible to shading heaviness when a certain critical point is met. This dissertation presents an investigation of the impact of partial shading and the critical point that reduce the susceptibility of shading heaviness. Photovoltaic string formed by series-connected photovoltaic modules is used in this research. The investigation of the P-V characteristic curve under different numbers of shaded modules and shading heaviness suggests that the photovoltaic string becomes insusceptible to shading heaviness when the shaded modules irradiance reaches a certain critical point. The critical point can vary based on the number of the shaded modules. The formulated equation in this research contributes to determining the critical point for different photovoltaic string sizes and numbers of shaded modules in the photovoltaic string.

LIST OF CONTENTS

LIST OF FIGURE

LIST OF TABLES

SYMBOLS AND ABBREVIATIONS

A	Diode ideality factor
$\mathbf{I_{PH}}$	Photo generated current
D	Duty cycle
$\mathbf{R_b}$	Beam Radiation
$\mathbf{R_d}$	Diffuse Radiation
$\mathbf{R_r}$	Reflected radiation
T	Temperature (K).
$\mathbf{R_t}$	Total solar radiation on tilted surface
$\mathbf{I_D}$	Diode current
$\mathbf{I_o}$	Diode reverse saturation current
I	Output current
$\mathbf{I_{sc}}$	Short-circuit current of a PV cell
J	Moment of inertia of the system in kg-m^2
K	Boltzmann's constant
$\mathbf{L_a}$	Self inductance of the armature winding
$\mathbf{P_{max}}$	Maximum power output of a PV string
$\mathbf{P_{string}}$	Output power of the PV string
q	Charge of an electron
$\mathbf{R_a}$	Armature resistance
$\mathbf{R_s}$	Series resistance
$\mathbf{V_T}$	Thermal voltage
$\mathbf{N_S}$	Number of cells

CHAPTER-1
INTRODUCTION

Conventional electrical power generation based on coal-fired power plants introduces carbon emissions which cause air pollution to be released into the Earth's atmosphere. To tackle this problem, renewable energy is employed as an alternative mode of electrical power generation. Among the renewable energy options, photovoltaic solar power is getting more and more popular nowadays due to its abundantly available and inexhaustible nature [1–5]. The non-involvement of mechanical or moving parts in a photovoltaic power system also makes it more preferable than other renewable energy options [6]. In 2016, around 75 GW of solar photovoltaic capacity was installed worldwide, which is almost a 50% growth from about 50 GW in 2015 [7,8]. The significant growth in photovoltaic power systems promotes the popularity of photovoltaic power system research among renewable energy researchers.

1.1 Solar Energy:

Energy is defined as capacity to produce an effect to do work. Energy has been an important component to meet the day to day needs of human beings. Human society require increasing amount of energy for industrial, commercial, domestic, agriculture, and transport uses. Different forms of energy are defined as primary and secondary energy, commercial and non commercial energy, renewable and non renewable energy.

1.1.1 Primary and Secondary energy:

Primary energy refers to all types of energy extracted or captured directly from natural resources. Primary energy can be further divided into two parts namely renewable and non renewable energy.

Primary energy is transformed into more convenient form of energy such as electricity, steam etc. these form of energy are called secondary energy.

1.1.2 Commercial and Non commercial energy:

Energy that is available in the market for a definite price is known as commercial energy. The most important forms of commercial energy are electricity, coal, refined petroleum products and natural gas.

Any kind of energy which is sourced within a community and its surrounding area, and which is not normally treated in the commercial market is termed as non commercial energy such as firewood, cattle dung, agriculture waste etc.

1.1.3 Renewable and non renewable energy:

Renewable energy is obtained from natural sources. These resources can be used to produce energy again and again eg. Solar energy, wind energy, tidal energy etc.

Non renewable resources cannot be replaced once they are used eg. Coal, oil, gas etc. these energy resources are limited and would be exhausted within prescribed period of time.

Solar energy and solar radiation-

The earth receives the solar energy in the form of solar radiation. These radiations comprising of ultra-violet, visible and infrared radiation. The amount of solar radiation that reaches any given location is dependent on several factors like geographic location, time of day, season, land scope and local weather. Because the earth is round, the sun rays strike the earth surface at different angles (ranging from 0° to 90°). When sun rays are vertical, the earth's surface gets maximum possible energy.

Most of the part of India receives 4 to 7 kWh of solar radiation per square meter per day. India receives solar energy equivalent more than 5000 trillion kWh per year.

1.2 Solar radiation (Direct, diffuse and total solar radiation):

The solar radiation that reaches the surface of the earth without being diffused is called direct beam solar radiation. It is measured by instrument named as pyrheliometer.

As sun light passes through the atmosphere, some part of it is absorbed, scattered and reflected by air molecule, water vapours, clouds, dust and pollutants. This is called diffuse solar radiation. The diffuse solar radiation does not have unique path.

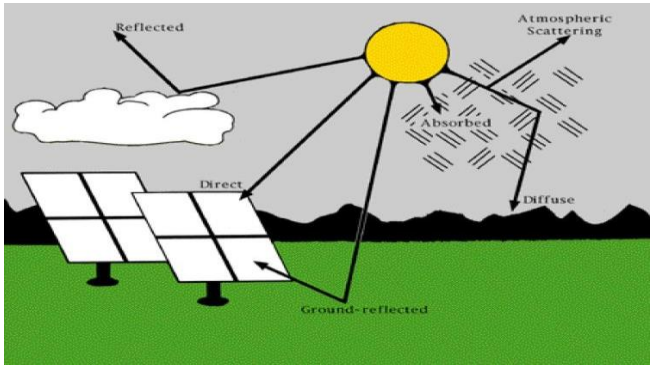

Figure. 1.1 Solar radiation

The sum of the direct and diffuse solar radiations is called total radiation or global solar radiation. Pyranometer is used for measuring the total radiation.

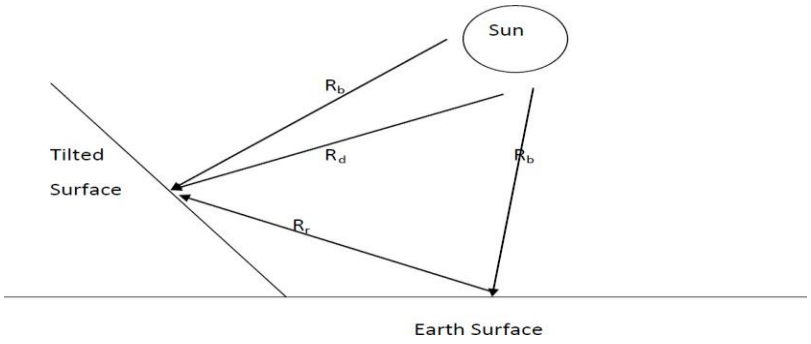

Figure.1.2 Direct, diffuse and total solar radiation

If,

R_b: Beam Radiation (direct solar radiation)

R_d: Diffuse Radiation (solar radiation after diffusion)

R_r: Reflected radiation (solar radiation after reflection from surface)

R_t: Total solar radiation on tilted surface

Then,

$$R_t = R_b + R_d + R_r \quad (1.1)$$

1.3 Photovoltaic modules:

Photovoltaic modules or solar panels are the most fundamental components in a photovoltaic power system which is used to convert solar energy to electrical power [9–13]. When a module is connected to a piece of measurement equipment, P-V characteristics will be obtained as illustrated in Figure 1.3[14]. The P-V characteristics demonstrate the electrical power delivered by the photovoltaic module at different voltages.

In the presence of the P-V characteristics, the maximum power of the photovoltaic module can be tracked. For instance, the marked point in Figure 1.3shows the highest point of the P-V characteristics, which represents the maximum power delivered by the photovoltaic module[15]. The maximum power of the photovoltaic module is always harvested from the photovoltaic module for electricity generation purposes [16]. Therefore, it is important to determine the P-V characteristics of a photovoltaic module so that the maximum power can be tracked and harvested from the photovoltaic module.

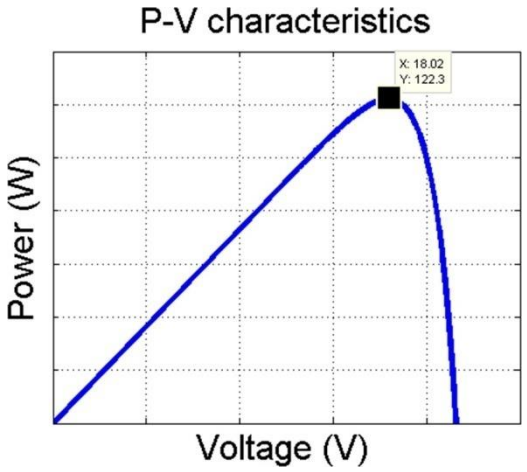

Figure 1.3. P-V characteristics of a photovoltaic module.

In a photovoltaic system, multiple photovoltaic modules are connected in series to form a photovoltaic string to achieve a required voltage and power output. To achieve an even higher power, these photovoltaic strings can be connected in parallel to form a photovoltaic array [17,18], as illustrated in Figure 1.4. In general, more than 1000 photovoltaic modules are employed in a megawatt-scale photovoltaic system to provide megawatts of electrical power production. These photovoltaic modules cannot only be connected in series as this will introduce an extremely high output voltage which makes it unfit for grid-connected inverters and energy storage purposes. Therefore, parallel connection is employed, as well as series connection, to connect these photovoltaic modules. Usually, multiple photovoltaic strings are formed by connecting multiple photovoltaic modules in series. These photovoltaic strings are then connected in parallel to form the photovoltaic array in the megawatts scale photovoltaic plant. Similar to the photovoltaic module, the P-V characteristics of a photovoltaic string/array need to be determined in order to track and harvest the maximum power from the photovoltaic string/array.

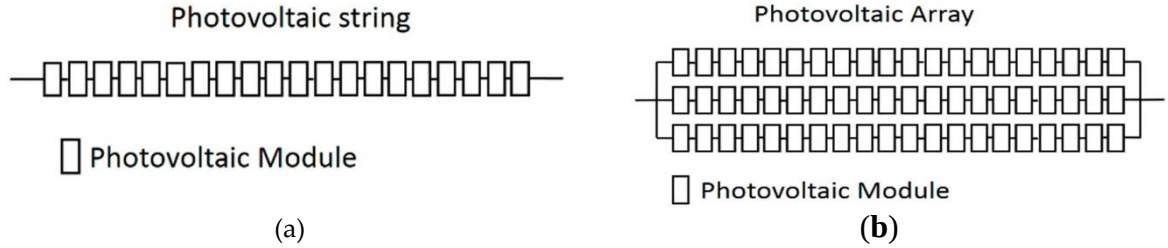

Figure 1.4. Photovoltaic system: (**a**) Photovoltaic string; (**b**) Photovoltaic array.

During a uniform irradiance condition, the P-V characteristics of a photovoltaic string exhibit one peak that resembles the P-V characteristics in Figure 1.3. The peak acts as the global peak which represents the maximum power of the photovoltaic string [19,20]. When partial shading takes place, multiple peaks appear on the P-V characteristics due to the use of a bypass diode [21–23]. Figure 1.5 shows the P-V characteristics of a photovoltaic string during a partial shading condition. The highest peak is the global peak which represents the maximum power of the photovoltaic string, while the others are the local peaks [24,25].

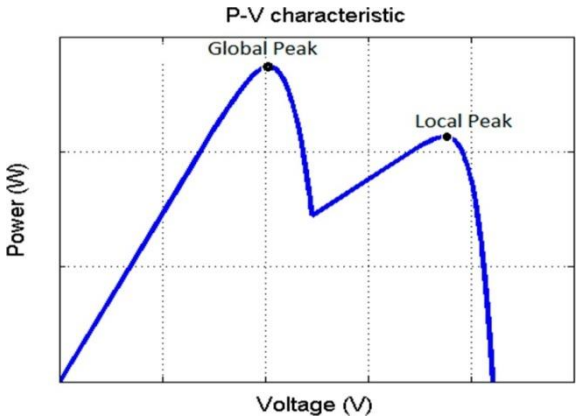

Figure 1.5. P-V characteristics of photovoltaic string under partial shading.

Apparently, a photovoltaic system is highly susceptible to partial shading [26–39]. During partial shading, the maximum power of a photovoltaic system can drop drastically, which significantly reduces the energy yield of the photovoltaic system. However, the susceptibility of partial shading to a photovoltaic system is not constant. The susceptibility of partial shading to a photovoltaic system can be varied due to the partial shading pattern and the connection employed to connect the photovoltaic modules in the photovoltaic system [26–29,32–38].

The experimental results in [26] suggested that under an identical partial shading pattern, the maximum power of a photovoltaic system should drop at a constant rate as the shading heaviness increases, as illustrated in Figure 1.6a. It means that under an identical partial shading pattern, a partially shaded photovoltaic system is always susceptible to the shading heaviness. This makes sense as the photovoltaic system relies on the solar irradiance to generate electrical power, and the maximum power of a partially shaded photovoltaic system should be lower and lower as the shading heaviness is getting heavier and heavier.

However, another phenomenon has been observed by S. Silvestre et al. [39]. S. Silvestre et al. discovered that a partially shaded photovoltaic system is not necessarily susceptible to

the shading heaviness. They discovered that the maximum power of a partially shaded photovoltaic system decreases as the shading heaviness increases, as presented by the researchers in [26–38]. However, when the shading heaviness reaches a certain critical point, the maximum power remains unchanged even if the shading heaviness is getting heavier and heavier from that critical point, as illustrated in Figure 1.6b. It means that the partially shaded photovoltaic system can become insusceptible to shading heaviness when the shading heaviness reaches a certain critical point. This finding is inspiring because a partially shaded photovoltaic system is commonly believed to always be susceptible to the shading heaviness.

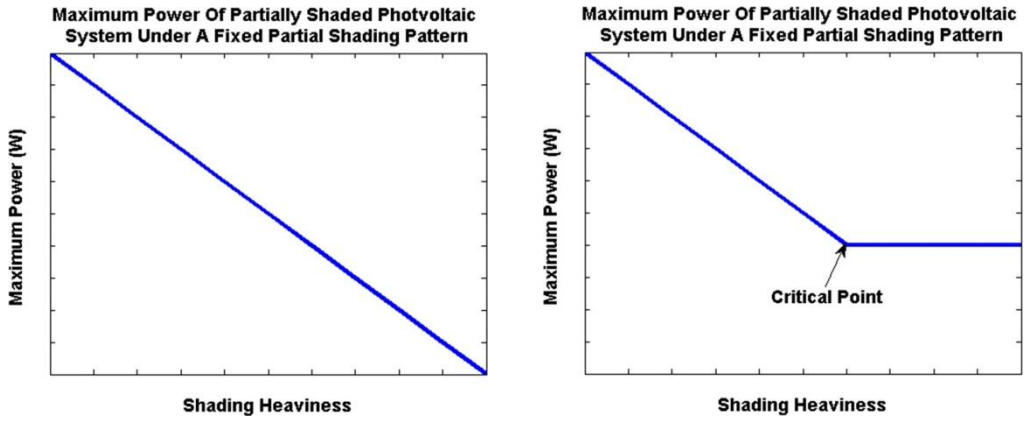

(a) (**b**)

Figure 1.6. Maximum power of a partially shaded photovoltaic system under a fixed partial shading pattern(**a**) as suggested by the experimental results in [26]; (**b**) as suggested by the experimental results in [39].

It is obvious that lots of research has been conducted on the impact of partial shading on the photovoltaic system throughout the years [26–38]. However, none of it has precisely presented the finding proposed in [39], which stated that the maximum power of a partially shaded photovoltaic system can become insusceptible to shading heaviness when the shading heaviness reaches a certain critical point. Therefore, it is a good area to further explore.

The finding proposed by [39] regarding the critical point is definitely inspiring. However, the experiment setup used in their research is a photovoltaic system that consists of nine photovoltaic modules only. They did not consider cases where a photovoltaic system consists of a greater number of photovoltaic modules. Besides that, the partial shading pattern and shading heaviness applied in their experiment are limited, which is insufficient to really conclude their finding. According to their result, the critical point can vary based on the number of shaded modules in the photovoltaic system. Therefore, an equation to determine the critical point for different numbers of shaded modules is highly expected. However, they

did not formulate an equation to determine the critical point. Furthermore, they did not verify whether the critical point is also applicable to different sized photovoltaic systems.

The aim of this research is to investigate the susceptibility of the shading heaviness to a partially shaded photovoltaic system and the critical point that decreases the susceptibility of shading heaviness using a photovoltaic system with a multiple number of photovoltaic modules and various partial shading conditions. Besides that, an equation to calculate the critical point is formulated in this research as well. Furthermore, the critical point equation is also verified with different sized photovoltaic systems.

With the increasingly environmental problems and shortages of traditional fossil fuels, solar energy as clean and renewable energy has attracted more and more attention. Photovoltaic power generation which has advantages of simplicity and convenience can directly convert solar energy to electrical energy. Coupled with the advancement of technology, such as improving conversion efficiency of solar cells and reducing the cost of devices, photovoltaic power generation is used more widely and has developed many different forms, including grid-connected or utility-interactive PV systems and stand-alone photovoltaic systems. But some undesirable problems such as hot spot and islanding effect occur correspondingly.

Hot spot occurs if the characteristics of solar cells mismatch are shaded or faulty, which reduces the short current of the shaded cell. Once the operating current of module or system exceeds the short current of the affected cell, the cell is forced into reverse bias and starts to consume the power generated by unshaded cells, resulting in overheating[42]. When the temperature of the shaded cell rises highly enough, the encapsulant, like EVA, will melt and the back sheet, like TPT, will be broken down, even leading to fire [43]. In general, bypass diodes are adopted to inhibit the shaded cell to crack and reduce the formation of hot spot. And the necessary parameters of bypass diodes and the number of cells in a string protected by a diode are determined by the parameters of normal cells [44].The typical group size is approximately 12–24 cells per bypass diode. However, these principles neglect whether or not the maximum heating power of the shaded cell can meet the requirement. It is also shown that bypass diodes are effective at preventing hot spot in short PV string lengths but cannot satisfy the demands in typical panel string lengths [45].

CHAPTER 2
LITERATURE SURVEY

2.1 LITERATURE REVIEW:

Considering the previous researches and the defects of principles of choosing bypass diodes, a new approach to study solar module is proposed and the influence of inhomogeneous illumination and incomplete shading of solar cells is investigated, respectively. For a certain circuit, the maximum power dissipation of the shaded cell happens at short-circuit conditions. Power dissipation of the shaded cell in different shading degrees is analyzed in order to find the worst working condition. As a result, the number of solar cells in a string should consider the worst case.

Sabrina Titri et al. (2017) described the The Maximum Power Point Tracking controller (MPPT) is a key element in Photovoltaic systems (PV). It is used to maintain the PV operating point at its maximum under different temperatures and sunlight irradiations. The goal of a MPPT controller is to satisfy the following performances criteria: accuracy, precision, speed, robustness and handling the partial shading problem when climatic changes variations occur. To achieve this goal, several techniques have been proposed ranging from conventional methods to artificial intelligence and bio-inspired methods. Each technique has its own advantage and disadvantage. In this context, we propose in this paper, a new Bio-inspired MPPT controller based on the Ant colony Optimization algorithm with a New Pheromone Updating strategy (ACO_NPU MPPT) that saves the computation time and performs an excellent tracking capability with high accuracy, zero oscillations and high robustness. First, the different steps of the design of the proposed ACO_NPU MPPT controller are developed. Then, several tests are performed under standard conditions for the selection of the appropriate ACO_NPU parameters (number of ants, coefficients of evaporation, archive size, etc.). To evaluate the performances of the obtained ACO_NPU MPPT, in terms of its tracking speed, accuracy, stability and robustness, tests are carried out under slow and rapid variations of weather conditions (Irradiance and Temperature) and under different partial shading patterns. Moreover, to demonstrate the superiority and robustness of the proposed ACO_NPU_MPPT controller, the obtained results are analyzed and compared with others obtained from the Conventional Methods (P&O_MPPT) and the

Soft Computing Methods with Artificial intelligence (ANN_MPPT, FLC_MPPT, ANFIS_MPPT, FL_GA_MPPT) and with the Bio Inspired methods (PSO) and (ACO) from the literature. The obtained results show that the proposed ACO_NPU MPPT controller gives the best performances under variables atmospheric conditions. In addition, it can easily track he global maximum power point (GMPP) under partial shading conditions[1].

Ehsanul Kabiret al. (2018) discussed the development of novel solar power technologies is considered to be one of many key solutions toward fulfilling a worldwide increasing demand for energy. Rapid growth within the field of solar technologies is nonetheless facing various technical barriers, such as low solar cell efficiencies, low performing balance-of systems (BOS), economic hindrances (e.g., high upfront costs and a lack of financing mechanisms), and institutional obstacles (e.g., inadequate infrastructure and a shortage of skilled manpower). The merits and demerits of solar energy technologies are both discussed in this article. A number of technical problems affecting renewable energy research are also highlighted, along with beneficial interactions between regulation policy frameworks and their future prospects. In order to help open novel routes with regard to solar energy research and practices, a future roadmap for the field of solar research is discussed[4].

Fatih Bayrak et al. (2017) presented the Photovoltaic (PV) technology becomes very popular with development of material science among the indispensable of solar energy in recent years. In this paper is investigated the electrical performance and thermodynamics analysis under the shading shapes and shading ratios of photovoltaics panels which have in 75 W power. The operating and electrical parameters of a photovoltaic panel are including cell temperature, overall heat loss coefficient, fill factor, etc. With this aim, an experimental set-up was constructed and serial experiments were done for different parameters such as shading ratio and positions. Three different cases of shading effects as cell, horizontal and vertical shading at different percentage. The results showed that the values of fill factor are also determined for the systems and effect of fill factor on the efficiencies is also evaluated. The shading makes important effect on energy and exergy efficiencies of the system and the most important effect is formed in case of horizontal shading. The maximum power loss was occurred at the shading rate 100% as 69.92% in cellular, 66.93% in vertical, 99.98% in horizontal shading[6].

Federica Cucchiella et al. (2017) used the New installed annual solar photovoltaic (PV) capacity was equal to 76.1 GW in 2016 (+49%), reaching the total of 305 GW around the world. PV sources are able to achieve a greater energy independence, to tackle the climate

change and to promote economic opportunities. This work proposes an economic analysis based on well-known indicators: Net Present Value (NPV), Discounted Payback Time (DPBT) and Levelized Cost of Electricity (LCOE). Several case studies are evaluated for residential households. They are based on three critical variables: plant size (1,2,3,4,5 and 6 kW), levels of insolation (1350, 1450 and 1550 kWh/(m^2×y)) and share of self-consumption (30%, 40% and 50%). The profitability is verified in all case studies examined in this work. The role of self-consumption, that is the harmonization between demanded and produced energy, is strategic in a mature market to improve financial performance. A sensitivity analysis, based on both electricity purchase and sales prices (critical variables), confirms these positive results. The Reduction in the Emissions of Carbon Dioxide (ER_{cd}) signifies an environmental improvement when a PV system is used as an alternative to a mix of fossil fuels. Finally, a policy proposal is examined based on a fiscal deduction of 50% fixing the period of deduction equal to 5 years.[7]

Anuja Ingle et al. (2017) discuss the various solar energy applications offer clean, environment friendly and exhaustive energy resources to human being. Solar system directly converts the sunlight energy into electrical energy through Photovoltaic (PV) module and indirectly through concentrated lenses. PV module configurations play vital role in improving the performance of the PV system. This paper discussed the impact of different configurations like series parallel (SP), total cross tied (TCT), Bridge link (BL) and honey comb (HC) on system performance. Attempts are also made to highlight the currents issues and challenges involved in solar system[9].

Soubhagya K.Das et. al.(2017) discuss the Photovoltaic (PV) systems are gaining popularity for both standalone and grid connected applications. These systems offer benefits of being static, modular, environmental friendly; and converts light from the Sun, which is perennial source of clean and green energy. The energy conversion in *PV* system is although instantaneous, yet less efficient because of optical and electrical losses. The optical loss caused by partial shading reduces a *PV* system output greatly, if not properly mitigated. The shading mitigation techniques are therefore an integral part of power conditioning unit of all large *PV* systems. These mitigation techniques ensure global peak operation of *PV* plant under undesirable condition of partial shading. Multitudes of such mitigation techniques are available in literature; though each one of them exhibits some vulnerability. This paper therefore intends to present state-of-art in existing shading mitigation techniques. The review presents rationale behind the reported techniques and compares them on some common parameters of control strategy, *granularity,* accuracy, tracking speed, complexity, efficiency

and number of sensors employed. This comprehensive review on shading mitigation techniques would certainly help researcher to select appropriate MPPT techniques for a given PV application[16].

Yu-Chen Liu et. al (2018) discuss an isolated photovoltaic micro-inverter for standalone and grid-tied applications is designed and implemented to achieve high efficiency. System configuration and design considerations, including the proposed active-clamp forward-fly back resonant converter for the DC-DC stage and a dual-frequency full-bridge inverter for the DC-AC stage, are analyzed and discussed. A prototype micro inverter system is built and tested. Experimental results verify the feasibility of the proposed system, which achieves 95% power conversion efficiency at full load[18].

Herrmann et al.[1997] presented an improved methodology for hot spot testing due to the shortages of two current hot spot tests and introduced the worst case power dissipation of the shaded cell but did not consider the great influence of radiation [46].

Silvestre et al.[2009] simulated solar cells and PV modules with bypass diodes working in partial shading conditions and verified with real measure data. A method on estimating the number of cells protected by bypass diode was proposed according to the correlation of the voltage not considering dissipated power of the shaded cell [47].

Quaschning and Hanitsch and Kawamura et al.[1996,2003] respectively, conducted a simulation research about the current and voltage of photovoltaic systems in partial shading [48, 49].

Bende et. al.[2014] performed a simulation study of the partially shaded cell by varying the breakdown voltage and the shunt resistance of cells and analyzed the effect of these parameters on the maximum power dissipation [50].

Fertig et al.[2011] investigated the impact of reverse breakdown of solar cells on the hot spot, simulated the distribution of the temperature of the shaded cell, and validated it with experimental data [51–53].

Alsayid et al.[2013] analyzed the effect of partial shading on the PV system but the results only contained inhomogeneous illumination and neglected incomplete shading [54–56].

CHAPTER 3

METHODOLOGY

A photovoltaic string consists of 4 photovoltaic modules and is used to conduct the experiment in this research. The photovoltaic modules have an open circuit voltage of 21.6 V, short circuit current of 7.34 A ideality factor of 1.5, and series resistance of 0 ohm. Temperature, T = 25°C is used for all the case studies in the experiment. Each photovoltaic module in the photovoltaic string has one bypass diode.

There are three experiment setups developed using the photovoltaic string, including 1 modules shaded, 2 modules shaded and 3 modules shaded setups.

Table 3.1 shows all the conditions that applied to every experimental setup. In the experiment, the P-V characteristics of every experimental setup under all the applied conditions are determined.

Table 3.1. Conditions applied to the experimental setups.

Conditions	**Unshaded Modules Irradiance (W/m^2)**	**Shaded Modules Irradiance (W/m^2)**
Condition 1	1200	1000
Condition 2	1200	800
Condition 3	1200	600
Condition 4	1200	400
Condition 5	1200	200
Condition 6	1200	100

A photovoltaic array that consists of parallel connected photovoltaic strings and is not used in this research. This is because a photovoltaic system with a higher degree of parallelism is less susceptible to partial shading [32]. Similar statements are also suggested in [33–40], which address the fact that a higher degree of parallelism in a photovoltaic

system can reduce the susceptibility of partial shading. Therefore, a photovoltaic array that consists of parallelism is not used in this research. Photovoltaic string that is in a series connected configuration is used in this research.

The random partial shading patterns with multiple shading heaviness are not used in this research. These partial shading patterns occur due to an uneven cloud distribution. It is more likely to be experienced by a megawatts scale photovoltaic plant. The area of the coverage of the photovoltaic string is not as big as a megawatts scale photovoltaic system. Therefore, the random partial shading patterns with multiple shading heaviness are not considered in this research.

There is not a standard rule for choosing the photovoltaic system size to conduct the partial shading experiment. The size can be chosen based on the designer and researcher preferences. For instance, Hiren Patel and Vivek Agarwal [26] chose photovoltaic arrays that consist of 300, 900, and 1000 photovoltaic modules; R. Ahmad et al. [29] chose photovoltaic arrays that consist of 20 and 25 photovoltaic modules; S. Silvestre et al. [39] chose a photovoltaic array consisting of nine photovoltaic modules, and so on. Regardless of the chosen size of the photovoltaic system, the experimental outcome should be applicable in certain ways to a megawatts scale photovoltaic plant as tacitly assumed among the researchers [26–39].

A photovoltaic string model is developed to carry out the experiment. A solar cell block from the Sim Electronics block set is used to develop the photovoltaic string model. This method of modelling has been used by J. C. Teo et al. to develop a photovoltaic string model [11]. They have conducted practical measurements to validate the photovoltaic string model in their research. Hence, it makes sense to use this method to develop the photovoltaic string model for the experiment.

The solar cell block is set to a five-parameter configuration m which is defined in Equations (3.1) and (3.2), where I is the output current, I_{PH} is the photo-generated current, I_O is the diode saturation current, V is the output voltage, R_S is the series resistance, N_S is the number of cells, V_T is the junction thermal voltage, A is the ideality factor, k is the Boltzman constant ($1.3806503 \times 10^{-23}$ J/K), T is the cell temperature, and q is the electron charge ($1.6021765 \times 10^{-19}$ C).

$$I = I_{PH} - I_0 exp\left(\frac{V+IR_S}{N_S V_T} - 1\right) \quad (3.1)$$

$$V_T = \frac{AKT}{q} \quad (3.2)$$

The short circuit current, open circuit voltage, series resistance, and ideality factor of the solar cell block are set according to the experiment requirements. To implement the bypass diode, the diode block from the Simscape block set is connected in antiparallel with the solar cell block, as shown in Figure 3.2.

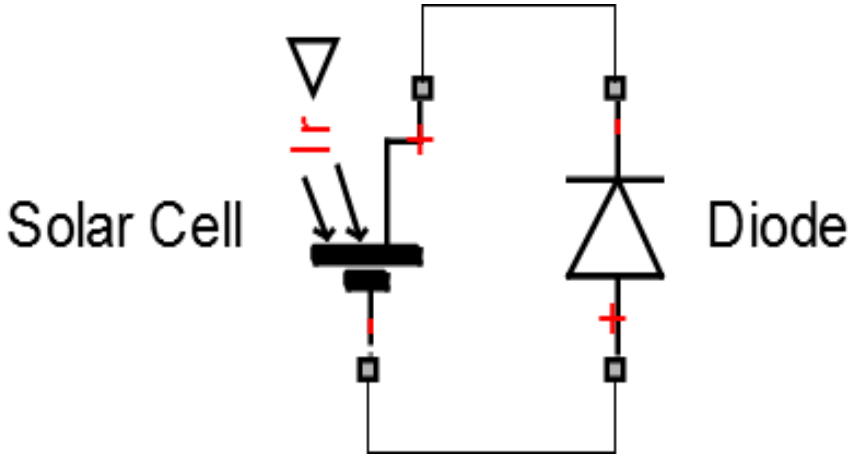

Figure 3.1. Solar cell block with bypass diode.

The architecture in Figure 3.1 represents a photovoltaic cell with a bypass diode. The architecture is duplicated to one sets, and these one sets of architecture are then connected in series to form a photovoltaic string model which consists of 4 photovoltaic modules that are required for the experiment. The photovoltaic string model is made into a single block known as PV string, as shown in Figure 3.2.

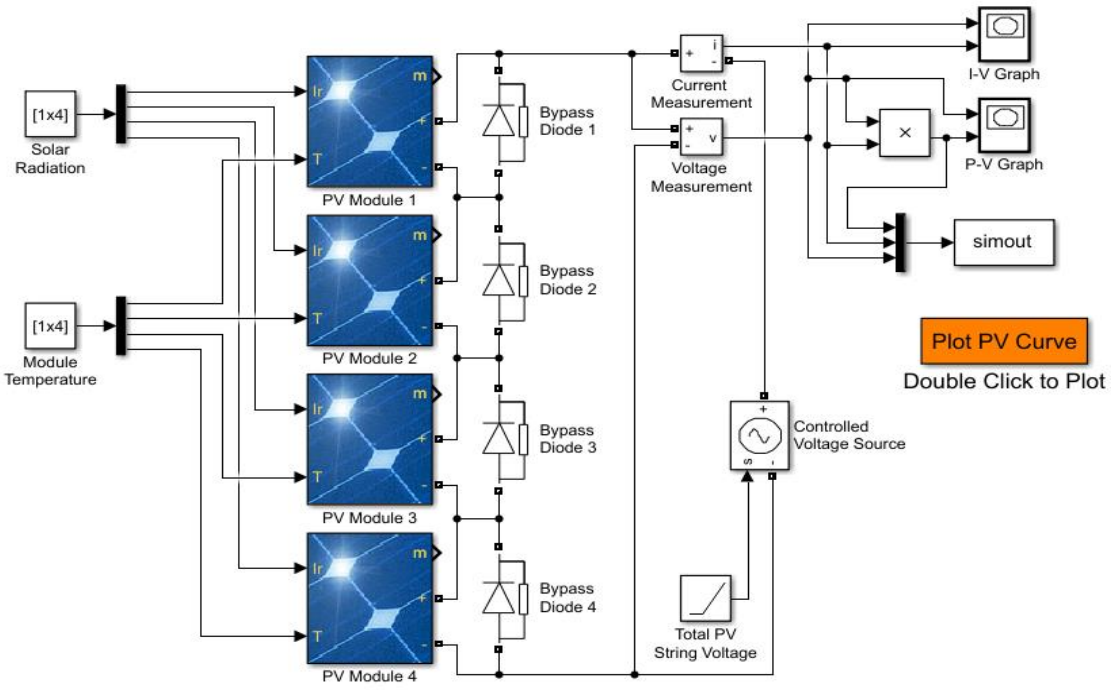

Figure 3.2. Photovoltaic string model.

Figure 3.2 shows the entire photovoltaic string model that was developed to carry out the experiment. The PV string block is the model for the photovoltaic string. It has 4 inputs which control the irradiance of every particular photovoltaic module in the photovoltaic string. The Control Unit block sets the unshaded modules irradiance, shaded modules irradiance, and number of the shaded modules in the PV string based on the parameter in the Unshaded Irr, Shaded Irr, and Shade Module block, respectively.

During the simulations, the Controlled Current Source block sweeps the output current of the photovoltaic string. The Voltage Sensor block measures the output voltage of the photovoltaic string. The Product block multiplies the output voltage and output current of the photovoltaic string to obtain the output power of the photovoltaic string. The To Workspace block sends the output power and output voltage of the photovoltaic string to the MATLAB (R2014a, MathWorks, Natick, MA, USA) workspace to plot the P-V characteristics curve.

Basically, the developed photovoltaic string model shown in Figure 3.2 is developed by cascading and extending the photovoltaic string model proposed by J. C. Teo et al. [11].

It is common practice to develop a larger scale photovoltaic system model by cascading and extending the validated small-scale photovoltaic system model [26]. The larger scale model that is developed by cascading and extending the validated small-scale model should give appropriate results for analysis purposes, as suggested by [26,39]. The method in [26] has also been applied by another researcher [29] to conduct a partial shading experiment.

The experiment can be conducted using the photovoltaic string model shown in Figure 3.2. To conduct the experiment for the three modules shaded setup, the Unshade Irr block is set to 1200 while the Shaded Module block is set to one. These settings configure the photovoltaic string to a three modules shaded setup with the unshaded modules irradiance fixed at 1200 W/m^2. The Shade Irr block is set to 1000 to apply the condition 1 in Table 3.2 to the one modules shaded setup. Simulation performed under these setting generates the P-V characteristics of the one modules shaded setup under condition 1. To obtain the P-V characteristics of the one modules shaded setup under all the conditions in Table 3.2, 6 simulations are performed with the Shade Irr block set to 100, 200, 400, 400, 600, 800 and 1000, respectively.

Similar procedures are applied to conduct the experiment for the two modules shaded, and three modules shaded setup. For instance, for the two modules shaded setup, the Unshade Irr block is set to 1200 while the Shade Module block is set to 1000-100 W/m^2. These settings configure the photovoltaic string to the two modules shaded setup with the unshaded module irradiance fixed at 1200 W/m^2. To obtain the P-V characteristics of the two modules shaded setup under all the conditions in Table 3.3, 6 simulations are performed with the Shade Irr block set to 100, 200, 400, 600, 800 and 900, respectively.

To conduct the experiment for the three modules shaded setup, the Unshade Irr block is set to 1200 while the Shade Modules block is set to 1000-100W/m^2. The simulations are performed with the Shade Irr block set to 100, 200,400, 600, 800 and 1000, respectively, to obtain the P-V characteristics of the three modules shaded setup under the Tables 3.2–3.4 show the parameters set in the model in Figure 3.2 to conduct the experiment for the one modules shaded, two modules shaded and three modules shaded setups.

Table 3.2. Parameters set in the model shown in Figure 4.1 to conduct the experiment for the one modules shaded setup

Condition Applied to the Experiment Setup	Temperature(^{0}C)	Parameter Set in Shade Module Block	Parameter Set in Unshade Irr Block	Parameter Set in Shade Irr Block
Condition 1	30	1	1200	1000
Condition 2	30	1	1200	800
Condition 3	30	1	1200	600
Condition 4	30	1	1200	400
Condition 5	30	1	1200	200
Condition 6	30	1	1200	100

Table 3.3. Parameters set in the model shown in Figure 4.2 to conduct the experiment for the two modules shaded setup

Condition Applied to the Experiment Setup	Temperature(^{0}C)	Parameter Set in Shade Module Block	Parameter Set in Unshade Irr Block	Parameter Set in Shade Irr Block
Condition 1	30	2	1200	1000
Condition 2	30	2	1200	800
Condition 3	30	2	1200	600
Condition 4	30	2	1200	400
Condition 5	30	2	1200	200
Condition 6	30	2	1200	100

Table 3.4. Parameters set in the model shown in Figure 4.3 to conduct the experiment for the three modules shaded setup

Condition Applied to the Experiment Setup	Temperature(^{0} C)	Parameter Set in Shade Module Block	Parameter Set in Unshade Irr Block	Parameter Set in Shade Irr Block
Condition 1	30	2	1200	1000
Condition 2	30	2	1200	800
Condition 3	30	2	1200	600
Condition 4	30	2	1200	400
Condition 5	30	2	1200	200
Condition 6	30	2	1200	100

The experiment considers lots of partial shading conditions, including lightly shaded, heavily shaded, a small number of modules shaded, a big number of modules shaded, and lots of shading heaviness conditions. These partial shading conditions pretty much cover all the possible partial shading conditions that might be experienced by a photovoltaic string at the site. Hence, the data collected in the experiment should be sufficient to conclude the critical points of a photovoltaic string, as well as to formulate the equation to determine the critical points of a photovoltaic string. However, more simulation work is required to conduct the experiment as it involves a huge number of partial shading conditions.

CHAPTER-4

RESULT

Figure 4.1 shows the P-V characteristics of the one modules shaded setup. Figure 4.1 represents the P-V characteristics when the shaded modules irradiance is between 1000 and 100 W/m^2. Considering the one modules shaded setup in Figure 4.1, the higher voltage peak of the P-V characteristics is higher than the lower voltage peak when the shaded module irradiance is 1000 W/m^2 .

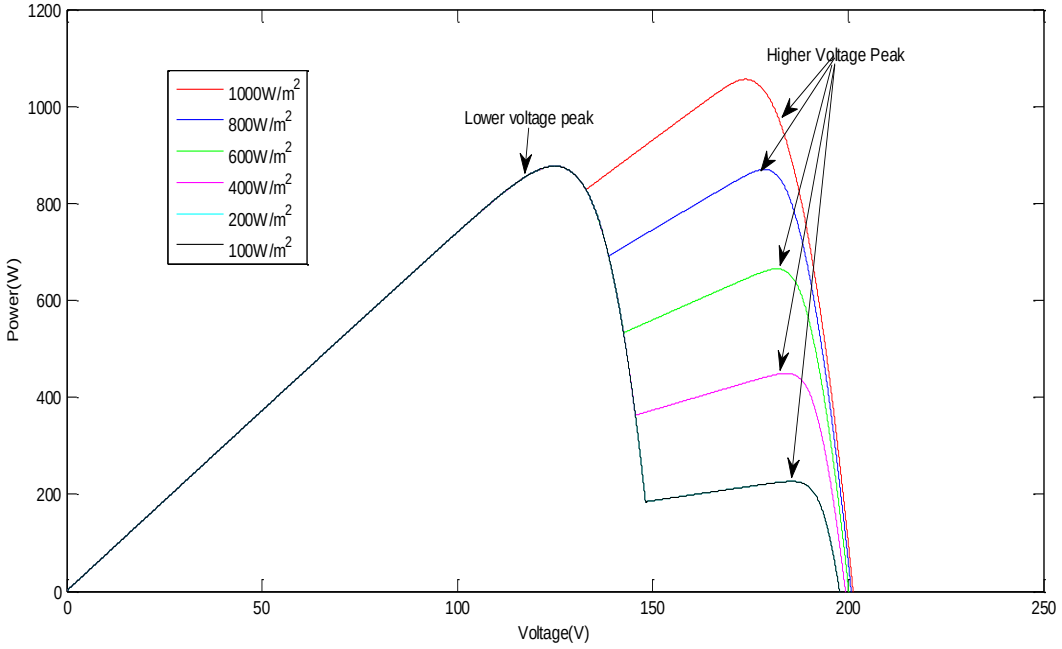

Figure 4.1. P-V characteristics of the one modules shaded setups: shaded modules irradiance is between 1000 and 100 W/m^2

Figure 4.2 shows the P-V characteristics of the two modules shaded setup. Figure 4.2 represents the P-V characteristics when the shaded modules irradiance is between 1000 and 100 W/m^2. Similar situations are observed in the two modules shaded setup shown in Figure 4.2, where the higher voltage peak acts as the global peak when the shaded modules irradiance is above a certain level. The higher voltage peak reduces as the shaded modules irradiance decreases.

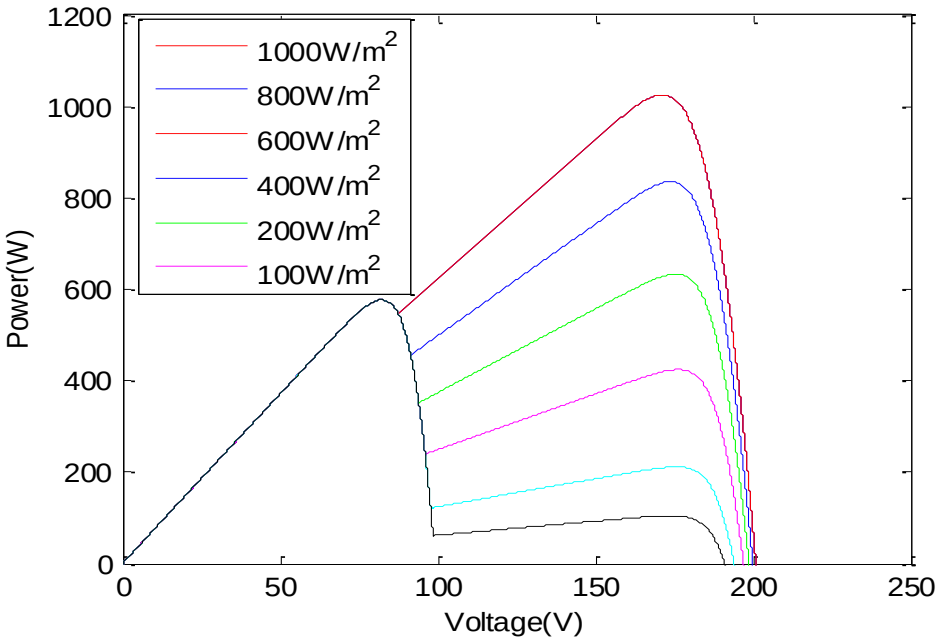

Figure 4.2. P-V characteristics of the two modules shaded setups: shaded modules irradiance is between1000 and 100 W/m^2

Figure 4.3 shows the P-V characteristics of the three modules shaded setup. The similar situation that is observed in the one and two modules shaded setups is also observed in the three module shaded setups shown in Figures 4.3 . The higher voltage peak acts as the global peak when the shaded modules irradiance is above a certain level.

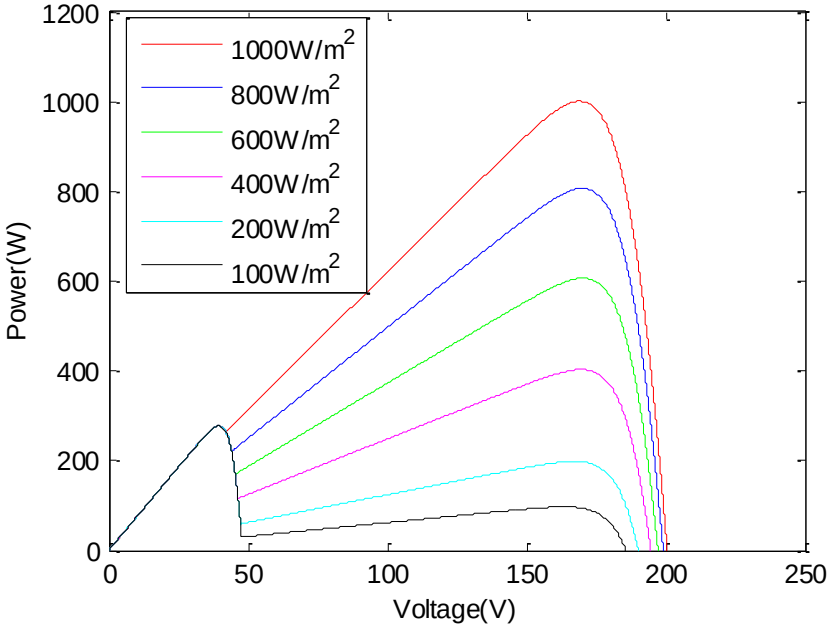

Figure 4.3. P-V characteristics of the three modules shaded setups:shaded modules irradiance is between 1000 and 100 W/m^2.

Tables 4.1– 4.3 are tabulated based on the data on the P-V characteristics of Figures 4.1–4.3 which show the maximum power and maximum power delivery voltage of all the experimental setups under the applied conditions.

Table 4.1. Maximum powers of the one modules shaded setup

Unshaded Module Irradiance (W/m^2)	**shaded Module Irradiance (W/m^2)**	**Maximum Power (W)**	**Delivery Voltage (V)**
1200	1000	1055.8	315
1200	800	876.8501	315
1200	600	876.8413	315
1200	400	876.8326	315
1200	200	876.8239	315
1200	100	876.8132	315

Table 4.2. Maximum powers of the two modules shaded setup

Unshaded Module Irradiance (W/m^2)	shaded Module Irradiance (W/m^2)	Maximum Power (W)	Delivery Voltage (V)
1200	1000	1025.6	315
1200	800	835.6950	204.23
1200	600	633.5483	315
1200	400	577.0554	315
1200	200	577.0380	315
1200	100	577.0293	315

Table 4.3. Maximum powers of the Three modules shaded setup

Unshaded Module Irradiance (W/m^2)	shaded Module Irradiance (W/m^2)	Maximum Power (W)	Delivery Voltage (V)
1200	1000	1001.10	315
1200	800	806.8980	315
1200	600	606.6071	315
1200	400	403.0876	315
1200	200	277.2680	315
1200	100	277.2550	315

By using the maximum powers and shaded modules irradiance in Table 4.1, a graph such as that illustrated in Figure 4.4 can be plotted. It shows the relationship between the maximum powers and the shaded modules irradiance of the one modules shaded setup.

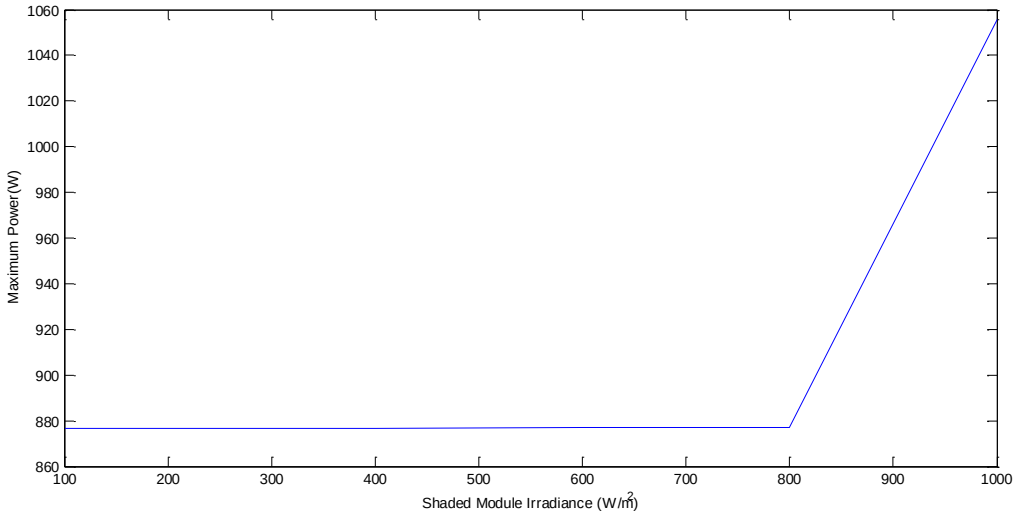

Figure 4.4. Maximum power versus shaded modules irradiance (one modules shaded).

Similar procedures are applied to Tables 4.2–4.3 to obtain the relationship between the maximum powers and the shaded modules irradiance for the 2 and 3 modules shaded setups. Figure 4.5 shows the relationship between the shaded modules irradiance and the maximum powers for all the experimental setups.

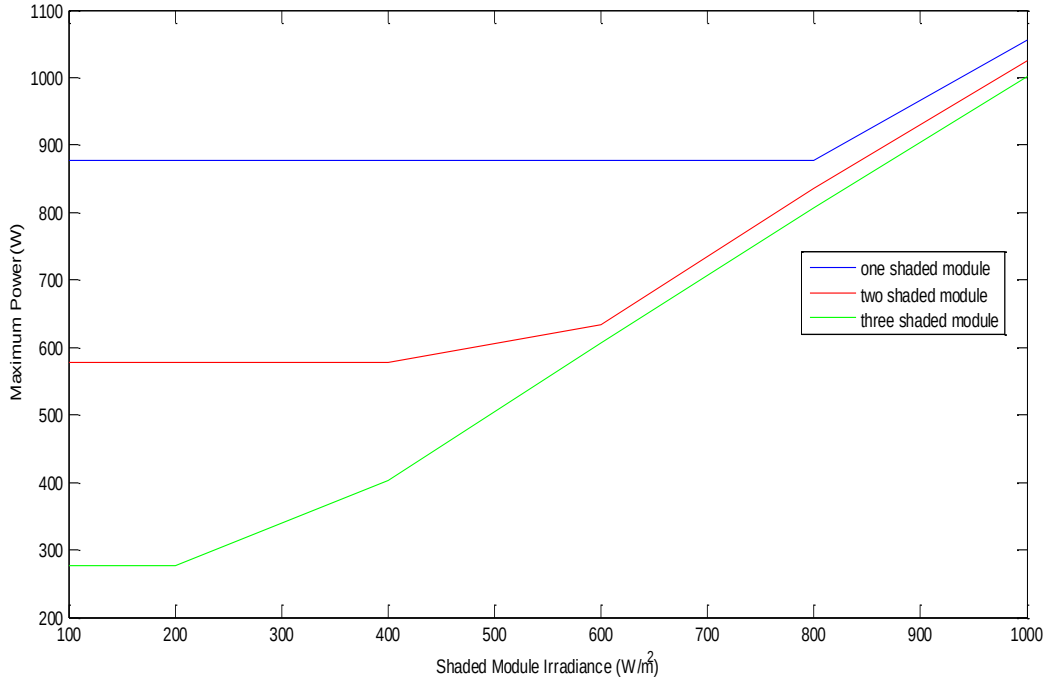

Figure 4.5. Maximum power versus shaded modules irradiance (all experiment setups).

CHAPTER-5

DISCUSSION

Considering the one modules shaded setup in Figure 4.1, the higher voltage peak of the P-V characteristics is higher than the lower voltage peak when the shaded module irradiance is 1000 W/m^2. Therefore, the higher voltage peak acts as the global peak that represents the maximum power of the photovoltaic string. The higher voltage peak reduces as the shaded modules irradiance decreases, as illustrated in Figure 4.1.When the shaded modules irradiance drops below 1000 W/m^2, the higher voltage peak eventually becomes lower than the lower voltage peak. Therefore, the lower voltage peak becomes the global peak that represents the maximum power of the photovoltaic string. Similar situations are observed in the two modules shaded setup shown in Figure 4.2, where the higher voltage peak acts as the global peak when the shaded modules irradiance is above a certain level. The higher voltage peak reduces as the shaded modules irradiance decreases. When the shaded modules irradiance drops below 800 W/m^2, the higher voltage peak eventually becomes lower than the lower voltage peak. Therefore, the lower voltage peak started to acts as the global peak which represents the maximum power of the photovoltaic string.

It is observed that the similar situations that are seen in the one and two modules shaded setups are also observed in three module shaded setups shown in Figures 4.3.The higher voltage peak acts as the global peak when the shaded modules irradiance is above a certain level. When the shaded modules irradiance drops below a certain level, the lower voltage peak started to acts as the global peak which represents the maximum power of the photovoltaic string.

Regardless of the number of shaded modules in the photovoltaic string, the higher voltage peak of the P-V characteristics reduces significantly as the shaded modules irradiance decreases. On the other hand, the lower voltage peak rarely changes as the shaded modules irradiance decreases. This is because the higher voltage peak of the P-V characteristics is formed by the shaded and unshaded photovoltaic modules in the photovoltaic string. Hence, the higher voltage peak is susceptible to the shading that is applied to the shaded photovoltaic modules. On the other hand, the lower voltage peak is formed by the unshaded modules in the photovoltaic string. Hence, the lower voltage peak is insusceptible to the shading applied to the shaded photovoltaic modules.

To apprehend this theory, consider the photovoltaic string in Figure 5.1. The photovoltaic string consists of four photovoltaic modules where two photovoltaic modules are unshaded and the other two photovoltaic modules are shaded, as illustrated in Figure 5.1. The unshaded photovoltaic modules generate 6.2 A and the shaded photovoltaic modules generate 3.01 A.

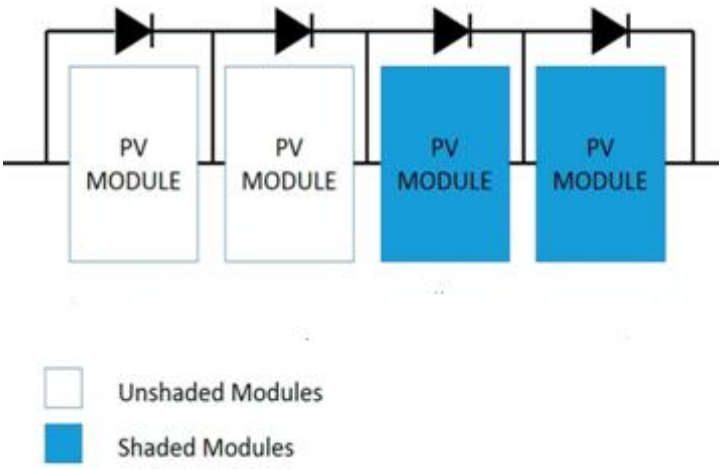

Figure 5.1. Photovoltaic string consisting of four photovoltaic modules.

When the load is drawing more than 3.01 A, the shaded photovoltaic modules are bypassed by the bypass diodes. Hence, the current generated by the unshaded photovoltaic modules is directed to the load without flowing through the shaded photovoltaic modules, as illustrated in Figure 5.2.Therefore, the I-V characteristics of the photovoltaic string above 3.01 A are formed by the unshaded photovoltaic modules only, as illustrated in Figure 5.3. Hence, variation in the shading heaviness on the shaded photovoltaic modules does not change the I-V characteristic at currents above 3.01 A.

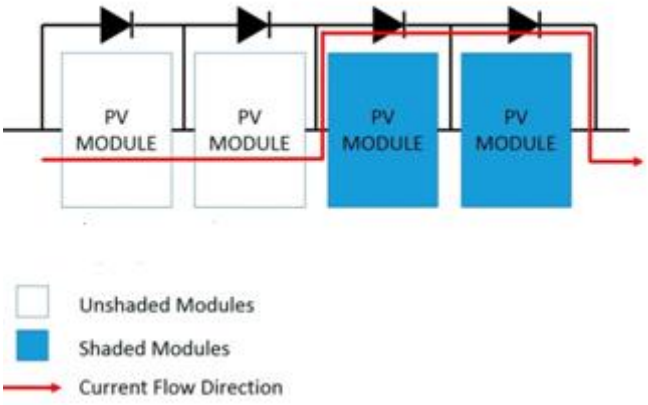

Figure 5.2. When the load is drawing more than 3.01 A.

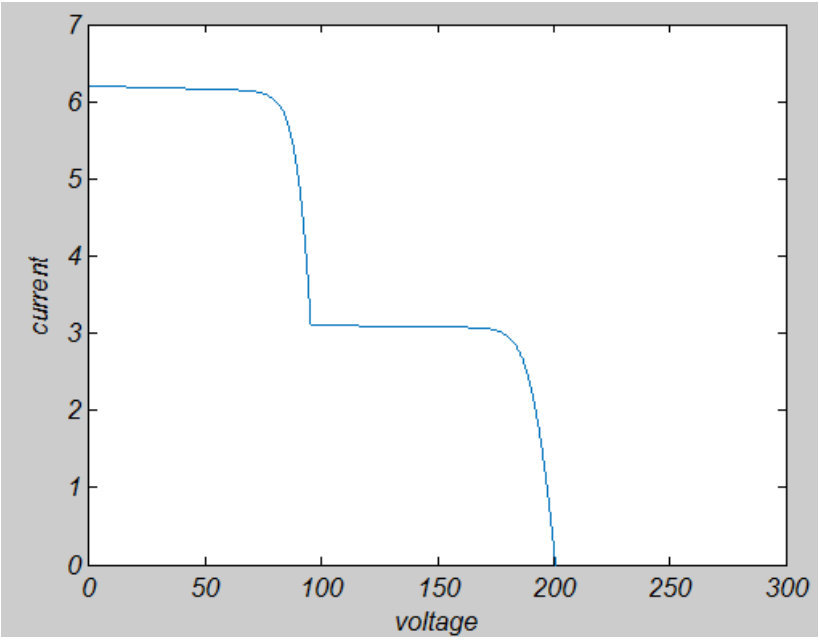

Figure 5.3. I-V characteristics above 3.01 A formed by unshaded modules.

When the load is drawing less than 3.01 A, the shaded photovoltaic modules are not bypassed by the bypass diodes. Hence, the current generated by the unshaded photovoltaic modules flow through the shaded photovoltaic modules, as illustrated in Figure 5.4. Therefore, the I-V characteristics of the photovoltaic string below 3.01 A are formed by the unshaded photovoltaic modules and shaded photovoltaic modules, as illustrated in Figure 5.5. Hence, the I-V characteristic below 3.01 A is susceptible to the shading heaviness on the shaded photovoltaic modules.

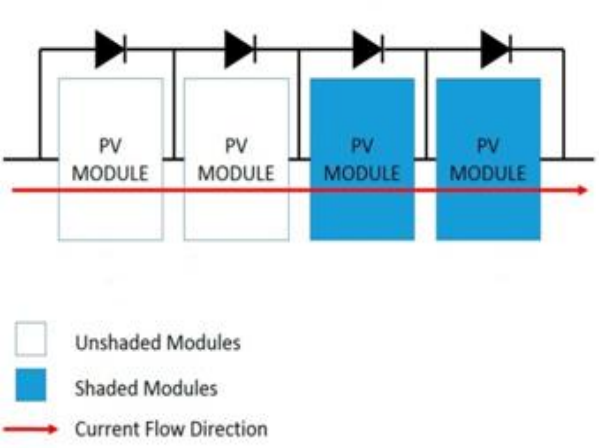

Figure 5.4. When the load is drawing less than 3.01 A.

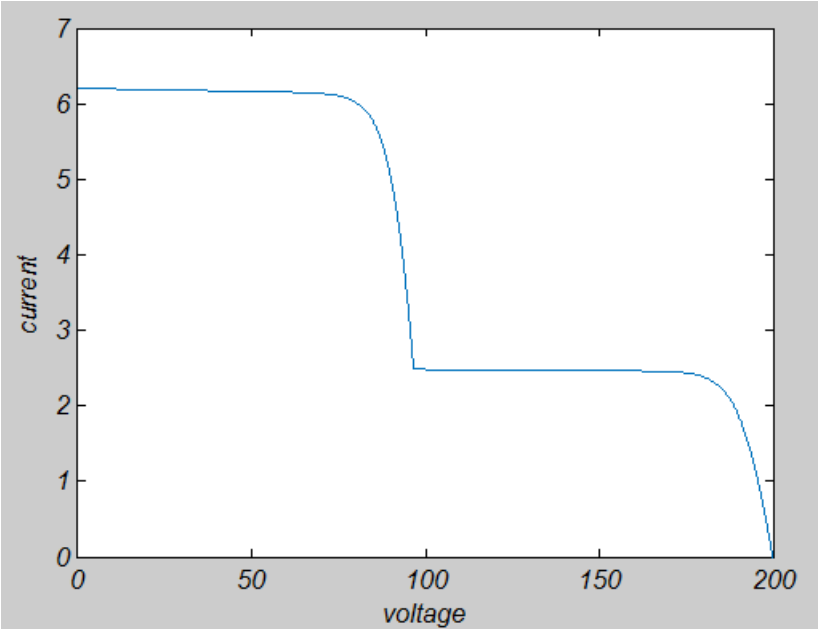

Figure 5.5. I-V characteristics below 3.01A formed by unshaded modules and shaded modules.

This proves that the higher voltage peak of the P-V characteristics is formed by the shaded and un shaded photovoltaic modules in the photovoltaic string. Hence, the higher voltage peak is susceptible to the shading on the shaded photovoltaic modules. On the other hand, the lower voltage peak is formed by the unshaded photovoltaic modules only, as concluded in Figure 5.6.

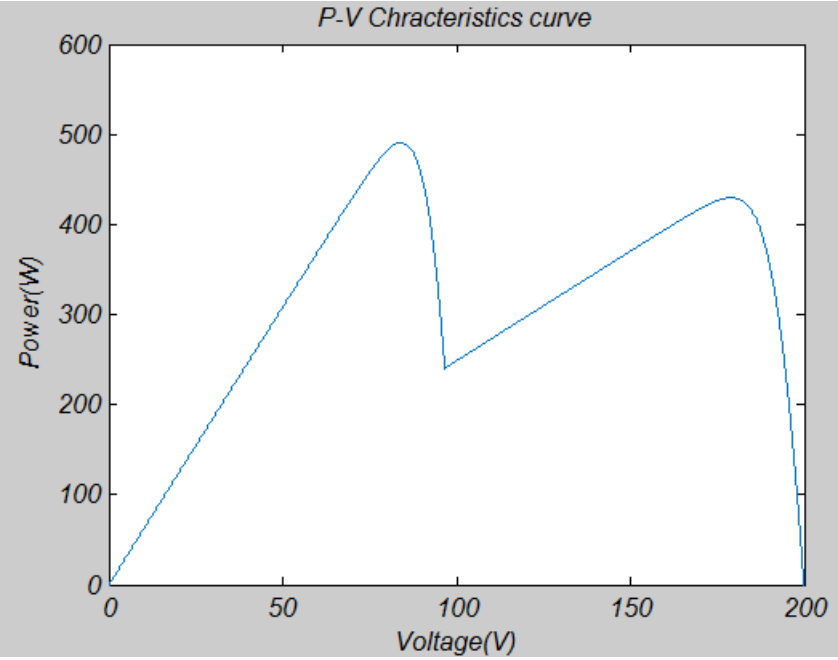

Figure 5.6. Higher and lower voltage peak of the P-V characteristics.

The maximum power does not necessarily deliver at a higher voltage. For instance, for the one modules shaded setup in Figure 4.1a, the maximum power is delivered at a higher voltage when the shaded modules irradiance is between 800 and 900 W/m^2, as illustrated in Figure 5.7. On the other hand, the maximum power is delivered at a lower voltage when the shaded modules irradiance is below or equal to 700 W/m^2, as illustrated in Figure 5.7. Similar situations are also observed in the two modules shaded and three modules shaded setups, as illustrated in Figures 4.2–4.3.When shaded modules irradiance is 800 to 900W/m^2 ,maximum power is delivered at higher voltage (174.4-177.5V) higher voltage peak of the P-V characteristics. When shaded modules irradiance is below 800W/m^2,maximum power is delivered at lower voltage(128.8-181.7V) lower voltage peak of the P-V characteristics.

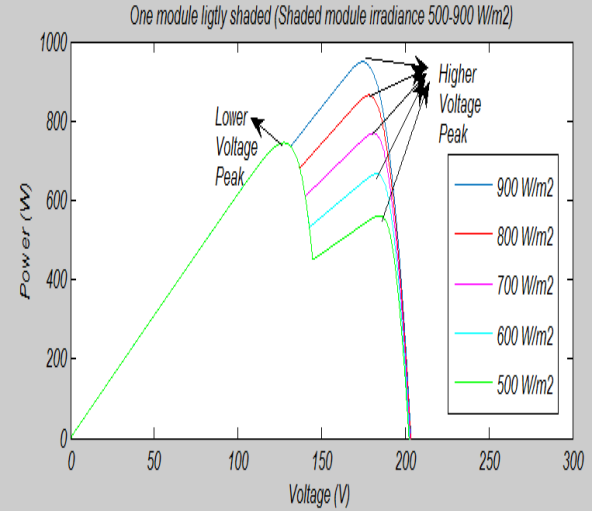

Figure 5.7. Delivery voltages for maximum power (one modules shaded setup).

Considering the two modules shaded setup in Figure 4.2, the maximum power is delivered at a lower voltage when the shaded modules irradiance is below or equal to the critical point of 500 W/m^2. Table 5.1 shows the critical point for the maximum power to deliver at a lower voltage. Equation (5.1) defines the equation to determine the critical point which is derived from Table 5.1.

$$CriticalPoint = -1000 \times \frac{\text{Number of shaded Modules}}{\text{Number of Total Modules}} + 900 \quad (5.1)$$

Table 5.1. Critical points for the maximum power to deliver at a lower voltage

Experiment Setup	**Shaded Modules Irradiance (W/m^2)**
One Modules Shaded	Less or equal to 650
Two Modules Shaded	Less or equal to 400
Three Modules Shaded	Less or equal to 150

To validate Equation (5.1), consider the photovoltaic string in Figure 5.8. The photovoltaic string consists of four photovoltaic modules where two photovoltaic module is unshaded and fixed at 1000 W/m^2. Another two photovoltaic module is shaded and is exposed to the irradiance of 100 to 900 W/m^2. Figures 5.10 and 5.11 show the simulation results of the photovoltaic string in Figure 5.8. The simulation results show that the maximum power is delivered at a lower voltage when the shaded module irradiance is below or equal to the critical point of 400 W/m^2. The critical point obtained from the simulation results resembles the critical point determined using Equation (5.1). Therefore, Equation (5.1) derived from the experiment is validated for different sizes of photovoltaic string.

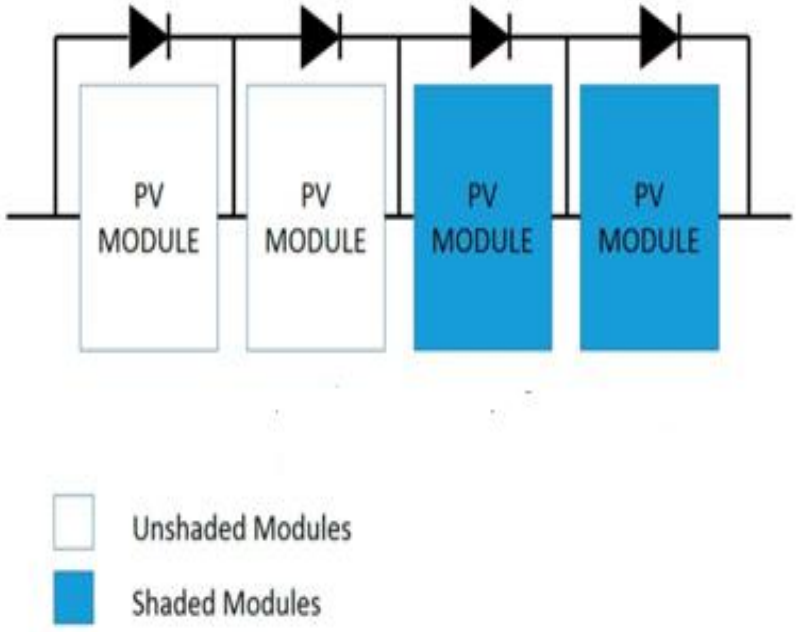

Figure 5.8. Photovoltaic string consisting of four photovoltaic modules.

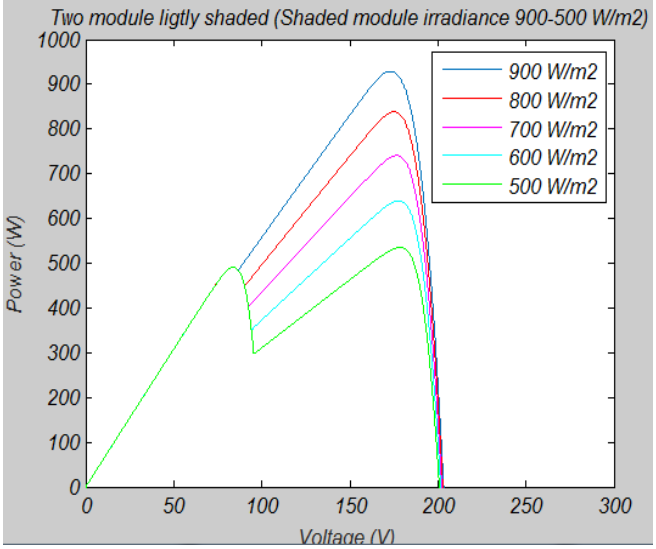

Figure 5.9. Simulated P-V characteristics of photovoltaic string in Figure 5.9—shaded module irradiance is between 500 and 900 W/m^2.

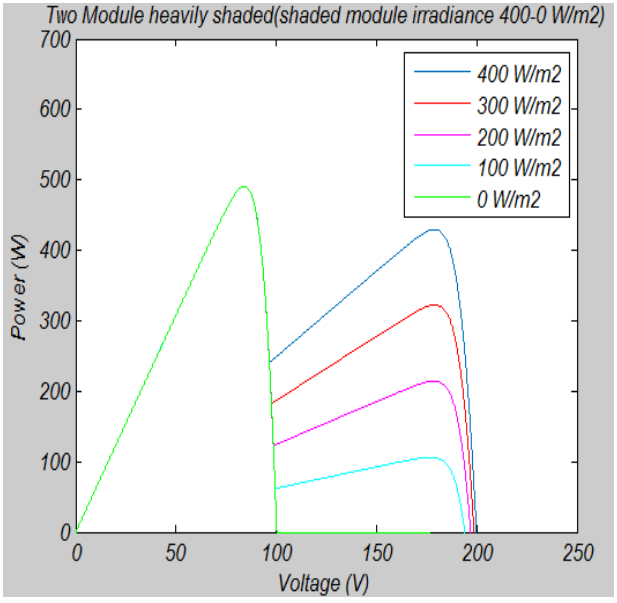

Figure 5.10. Simulated P-V characteristics of photovoltaic string in Figure 5.9—shaded module irradiance is between 0 and 400 W/m^2.

Maximum power is delivered at higher voltage when the shaded modules irradiance is 500-900W/m^2. Maximum power is delivered at lower voltage when the shaded modules irradiance is 100-400 W/m^{2}Hence, Equation (5.1) is applicable to photovoltaic string with

a small number of photovoltaic modules (two photovoltaic modules) and photovoltaic string with a big number of photovoltaic modules (20 photovoltaic modules). It shows that the critical point of large photovoltaic string and small photovoltaic string is not different in nature as they can both be determined using the same equation (Equation (5.1)). Therefore, Equation (5.1) should be applicable to any size of photovoltaic string. It should be applicable to the existing photovoltaic plants that consist of a huge number of photovoltaic modules because a megawatts scale photovoltaic plant consists of parallel connected photovoltaic strings. Equation (5.1) should also be suitable to determine the critical point of every photovoltaic string in the megawatts scale photovoltaic plant.

Consider the three modules shaded setup in Figure 4.3, where the maximum power drops significantly from 949.03 watts to 769 watts as the shaded modules irradiance drops from 1000 to 700 W/m^2. This is an 18.96% drop in the maximum power, which is an approximately 6.22% drop for every 100 W/m^2 drop in the shaded module irradiance. However, the maximum power rarely drops when the shaded modules irradiance is below or equal to 700 W/m^2. When the shaded modules irradiance drops from 700 to 0 W/m^2, the maximum power drops from 769 watts to 744.23 watts, which is only a 3.2% drop in the maximum power. It is an approximately 0.45% drop for every 100 W/m^2 drop in the shaded module irradiance. These results show that the maximum power is susceptible to the shading on the shaded modules when the shaded modules irradiance is above the critical point determined by Equation (5.1). The maximum power becomes insusceptible to the shading on the shaded modules when the shaded modules irradiance is below or equal to the critical point determined by Equation (5.1).

Similar situations are observed in the two modules shaded and three modules shaded setups. For instance, for the three modules shaded setup in Figure 4.3, the maximum power drops significantly from 912.4 watts to 235.7 watts as the shaded modules irradiance drops from 1000 to 100 W/m^2. This is equivalent to an approximately 8.24% drop in the maximum power for every 100 W/m^2 drop in the shaded module irradiance. However, the maximum power rarely drops when the shaded modules irradiance is less or equal to 100 W/m^2, which is the critical point determined by Equation (3). When the shaded modules irradiance drops from 100 to 0 W/m^2, the maximum power drops from 235.7 watts to 235.7 watts, which is only a

0 % drop in the maximum power for every 100 W/m^2 drop in the shaded module irradiance. Therefore, the shading on the shaded modules does not necessarily cause a high impact to the maximum power of the photovoltaic string. It depends on the number of shaded modules as well as the shading heaviness on the shaded modules. The maximum power is very susceptible to the shading on the shaded modules when the shaded modules irradiance is above the critical point determined by Equation (5.1). When the shaded modules irradiance is below or equal to the critical point, the maximum power of the photovoltaic string become insusceptible to the shading on the shaded modules. These findings address the condition when the photovoltaic string is susceptible to shading.

The experimental results are incomparable to those of other researchers presented in [26–39]. This is because the photovoltaic configuration, photovoltaic string size, and partial shading conditions applied in their experiments are different from this research. A similar issue is also restricting other researchers to compare their results with different research. However, the results in this research pretty much resemble the experimental results proposed by S. Silvestre et al. [39], which suggest that the maximum power of a photovoltaic system becomes insusceptible to the shading on the shaded modules when the shaded modules irradiance reaches a certain critical point.

The critical point calculation can contribute to the dynamical photovoltaic system reconfiguration mechanism. The dynamical photovoltaic system reconfiguration mechanism is used to reconfigure the photovoltaic modules connection in the photovoltaic system on a real time basis to tackle partial shading [40,41]. If the critical point is known, some unnecessary reconfiguration work can be reduced as the photovoltaic system become insusceptible to shading heaviness when the critical point is met. Elimination of unnecessary reconfiguration could reduce the stress of the charge controller of the energy storage. The proposed critical point calculation can contribute to the development of IEEE and IEC photovoltaic system standards, therefore leading to policy implementation wherever the standards are adopted. This research also provide opportunities to achieve the clean energy sustainable development goals (SDGs). Photovoltaic system research presented in this research can contribute to the improvement of renewable energy technology which can aid achievement of the Affordable and Clean Energy and Climate Action goal of the SDGs.

CHAPTER-7

CONCLUSION

Photovoltaic systems are highly susceptible to partial shading. The maximum power of a photovoltaic system can reduce drastically when partial shading takes place. The susceptibility of partial shading can vary based on the partial shading patterns, shading heaviness, and the configuration employed in connecting all the photovoltaic modules in the photovoltaic system. Under a fixed configuration and partial shading pattern, the maximum power of a partially shaded photovoltaic system is tacitly assumed to decrease at a constant rate as the shading heaviness increases. This tacit assumption is proposed based on the functionality of a photovoltaic system that relies on solar irradiance to generate electrical power. However, some researchers discovered that the maximum power under a fixed configuration and partial shading pattern can be highly insusceptible to shading heaviness when a certain critical point is met. Furthermore, the critical point can vary based on the number of shaded modules in a photovoltaic system. The novelty of this research includes the formulation of the equation to determine the critical point that is applicable to different photovoltaic system sizes and numbers of shaded modules in a photovoltaic system. Besides that, the equation has been verified with different sized photovoltaic systems as well. When 20% of photovoltaic modules in the photovoltaic system are shaded under an identical partial shading pattern, the maximum power drops by approximately 6.22% for every 100 W/m^2 drop in the shaded module irradiance as the shaded modules irradiance lies between 1000 and 700 W/m^2. However, when the shaded modules irradiance lies between 700 and 0 W/m^2, the maximum power drops only by 0.45% for every 100 W/m^2 drop in the shaded module irradiance. This means that the photovoltaic system becomes insusceptible to shading heaviness as the shaded modules irradiance reaches a critical point of 700 W/m^2. Some cases applied to 40%, 60%, and 80% of photovoltaic modules are shaded. The critical points of 40%, 60%, and 80% photovoltaic modules shaded are 500, 300, and 100 W/m^2, respectively. The critical point varies as the number of shaded modules changes. However, it is determinable using the equation formulated in this research. The proposed critical point calculation can contribute to the dynamical photovoltaic system reconfiguration mechanism.

If the critical point is known, some unnecessary reconfiguration switching can be reduced as the photovoltaic system become insusceptible to shading heaviness when the critical point is met.

REFERENCES

[1] Titri, S.; Larbes, C.; Toumi, K.Y.; Benatchba, K. A new MPPT controller based on the Ant colony optimization algorithm for Photovoltaic systems under partial shading conditions. Appl. Soft. Comput. 2017, 58, 465–479.[CrossRef]

[2] Pandeya, A.K.; Hossain, M.S.; Tyagi, V.V.; Rahim, N.A.; Selvaraj, J.A.; Sari, A. Novel approaches and recent developments on potential applications of phase change materials in solar energy. Renew. Sustain. Energy Rev. 2018, 82, 281–323. [CrossRef]

[3] Ozoegwu, C.G.; Mgbemene, C.A.; Ozor, P.A. The status of solar energy integration and policy in Nigeria. Renew. Sustain. Energy Rev. 2017, 70, 457–471. [CrossRef]

[4] Kabir, E.; Kumar, P.; Kumar, S.; Adelodun, A.A.; Kim, K. Solar energy: Potential and future prospects. Renew. Sustain. Energy Rev. 2018, 82, 894–900. [CrossRef]

[5] Kannan, N.; Vakeesan, D. Solar energy for future world: A review. Renew. Sustain. Energy Rev. 2016, 62,1092–1105. [CrossRef]

[6] Bayrak, F.; Ertürk, G.; Oztop, H.F. Effects of partial shading on energy and exergy efficiencies for photovoltaic panels. J. Clean. Prod. 2017, 164, 58–69. [CrossRef]

[7] Cucchiella, F.; D'Adamo, I.; Gastaldi, M. Economic analysis of a photovoltaic system: A resource for residential households. Energies 2017, 10, 814. [CrossRef]

[8] Rosa, C.B.; Rediske, G.; Rigo, P.D.; Wendt, J.F.M.; Michels, L.; Siluk, J.C.M. Development of a computational tool for measuring organizational competitiveness in the photovoltaic power plants. Energies 2018, 11, 867.[CrossRef]

[9] Ingle, A.; Sangotra, D.I.; Chadge, R.B.; Thorat, P. Module configurations in photovoltaic system: A review. Mater. Today Proc. 2017, 4, 12625–12629. [CrossRef]

[10] Syafiq, A.; Pandey, A.K.; Adzman, N.N.; Rahim, N.A. Advances in approaches and methods for self-cleaning of solar photovoltaic panels. Sol. Energy 2018, 162, 597–619. [CrossRef]

[11] Teo, J.C.; Tan, R.H.G.; Mok, V.H.; Ramachandaramurthy, V.K.; Tan, C.K. Effects of bypass diode configurations to the maximum power of photovoltaic module. Int. J. Smart Grids Energy 2017, 6, 225–232. [CrossRef]

[12] Siecker, J.; Kusakana, K.; Numbi, B.P. A review of solar photovoltaic systems cooling technologies.Renew. Sustain. Energy Rev. 2017, 79, 192–203. [CrossRef]

[13] Hazarika, K.; Choudhury, P.K. Automatic monitoring of solar photovoltaic (SPV) module. Mater. Today Proc. 2017, 4, 12606–12609. [CrossRef]

[14] Dolara, A.; Lazaroiu, G.C.; Leva, S.; Manzolini, G. Experimental investigation of partial shading scenarios on PV (photovoltaic) modules. Energy 2013, 55, 466–475. [CrossRef]

[15] Maghami, M.R.; Hizam, H.; Gomes, C.; Radzi, M.A.; Rezadad, M.I.; Hajighorbani, S. Power loss due to soiling on solar panel: A review. Renew. Sustain. Energy Rev. 2016, 59, 1307–1316. [CrossRef]

[16] Das, S.K.; Verma, D.; Nema, S.; Nema, R.K. Shading mitigation techniques: State-of-the-art in photovoltaic applications. Renew. Sustain. Energy Rev. 2017, 78, 369–390. [CrossRef]

[17] Wang, Y.; Li, Y.; Ruan, X. High accuracy and fast speed MPPT methods for PV string under partially shaded conditions. IEEE. Trans. Ind. Electron. 2016, 63, 235–245. [CrossRef]

[18] Liu, Y.; Chen, M.; Yang, C.; Kim, K.A.; Chiu, H. High-Efficiency Isolated Photovoltaic Microinverter Using Wide-Band Gap Switches for Standalone and Grid-Tied Applications. Energies 2018, 11, 569. [CrossRef]

[19] Bouselhama, L.; Hajjia, M.; Hajji, B.; Boualia, H. A New MPPT-based ANN for Photovoltaic System under Partial Shading Conditions. Energy Procedia 2017, 111, 924–933. [CrossRef]

[20] Eldahaba, Y.E.A.; Saad, N.H.; Zekry, A. Enhancing the tracking techniques for the global maximum power point under partial shading conditions. Renew. Sustain. Energy Rev. 2017, 73, 1173–1183. [CrossRef]

[21] Lia, G.; Jinb, Y.; Akramb, M.W.; Chen, X.; Ji, J. Application of bio-inspired algorithms in maximum power point tracking for PV systems under partial shading conditions—A review. Renew. Sustain. Energy Rev. 2018,81, 840–873. [CrossRef]

[22] Chaieb, H.; Sakly, A. A novel MPPT method for photovoltaic application under partial shaded conditions. Sol. Energy 2018, 159, 291–299. [CrossRef]

[23] Belhachat, F.; Larbes, C. Global maximum power point tracking based on ANFIS approach for PV array configurations under partial shading conditions. Renew. Sustain. Energy Rev. 2017, 77, 875–889. [CrossRef]

[24] Rezka, H.; Fathy, A.; Abdelaziz, A.Y. A comparison of different global MPPT techniques based on meta-heuristic algorithms for photovoltaic system subjected to partial shading conditions. Renew. Sustain. Energy Rev. 2017, 74, 377–386. [CrossRef]

[25] Mohapatra, A.; Nayak, B.; Das, P.; Mohanty, K.B. A review on MPPT techniques of PV system under partial shading condition. Renew. Sustain. Energy Rev. 2017, 80, 854–867. [CrossRef]

[26] Patel, H.; Agarwal, V. MATLAB-based modeling to study the effects of partial shading on PV array characteristics. IEEE. Trans. Energy Convers. 2008, 23, 302–310. [CrossRef]

[27] Bingöl, O.; Özkaya, B. Analysis and comparison of different PV array configurations under partial shading conditions. Sol. Energy 2018, 160, 336–343. [CrossRef]

[28] Bana, S.; Saini, R.P. Experimental investigation on power output of different photovoltaic array configurations under uniform and partial shading scenarios. Energy 2017, 127, 438–453. [CrossRef]

[29] Ahmad, R.; Murtaza, A.F.; Sher, H.A.; Shami, U.T.; Olalekan, S. An analytical approach to study partial shading effects on PV array supported by literature. Renew. Sustain. Energy Rev. 2017, 74, 721–732. [CrossRef]

[30] Teo, J.C.; Tan, R.H.G.; Mok, V.H. Investigation of shading characteristics of mono-crystalline and poly-crystalline photovoltaic modules connected in series. Appl. Mech. Mater. 2015, 785, 220–224. [CrossRef]

[31] Lua, F.; Guo, S.; Walsh, T.M.; Aberle, A.G. Improved PV module performance under partial shading conditions. Energy Procedia 2013, 33, 248–255. [CrossRef]

[32] Ramaprabha, R.; Mathur, B.L. A comprehensive review and analysis of solar photovoltaic array configurations under partial shaded conditions. Int. J. Photoenergy. 2012, 2012. [CrossRef]

[33] Tian, H.; Mancilla–David, F.; Ellis, K.; Muljadi, E.; Jenkins, P. Determination of the optimal configuration for a photovoltaic array depending on the shading condition. Sol. Energy 2013, 95, 1–12. [CrossRef]

[34] Reiter, R.D.; Michels, L.; Pinheiro, J.R.; Reiter, R.A.; Oliveira, S.V.G.; Péres, A. Comparative analysis of series and parallel photovoltaic arrays under partial shading

conditions. In Proceedings of the 10th IEEE/IAS International Conference on Industry Applications, Fortaleza, Brazil, 5–7 November 2012.

[35] Elserougi, A.A.; Abdel-Khalik, A.S.; Massoud, A.M.; Ahmed, S. A grid-connected switched PV array.In Proceedings of the 41st Annual Conference of the IEEE Industrial Electronics Society, Yokohama, Japan, 9–12 November 2015.

[36] Khatoon, S.; Ibraheem; Jalil, M.F. Analysis of solar photovoltaic array under partial shading conditions for different array configrations. In Proceedings of the IEEE International Conference on Innovative Applications of Computational Intelligence on Power, Energy and Controls with their Impact on Humanity, Ghaziabad, India, 28–29 November 2014.

[37] Boukenoui, R.; Bradai, R.; Salhi, H.; Mellit, A. Modeling and simulation of photovoltaic strings under partial shading conditions using Matlab/Simscape. In Proceedings of the IEEE International Conference on Clean Electrical Power, Taormina, Italy, 16–18 June 2015.

[38] Abdulazeez, M.; Iskender, I. Simulation and experimental study of shading effect on series and parallel connected photovoltaic PV modules. In Proceedings of the 7th IEEE International Conference on Electrical and Electronics Engineering, Bursa, Turkey, 1–4 December 2011.

[39] Silvestre, S.; Boronat, A.; Chouder, A. Study of bypass diodes configuration on PV modules. Appl. Energy 2009, 86, 1632–1640. [CrossRef]

[40] Carotenuto, P.L.; della Cioppa, A.; Marcelli, A.; Spagnuolo, G. An evolutionary approach to the dynamical reconfiguration of photovoltaic fields. Neurocomputing 2015, 170, 393–405. [CrossRef]

[41] Sanseverino, E.R.; Ngoc, T.N.; Cardinale, M.; Vigni, V.L.; Musso, D.; Romano, P.; Viola, F. Dynamic programming and Munkres algorithm for optimal photovoltaic arrays reconfiguration. Sol. Energy 2015, 122, 347–358. [CrossRef]

[42] Standard I. 61215, Crystalline Silicon Terrestrial Photovoltaic (PV) Modules—Design Qualification and Type Approval, 2005.

[43] H. Yoshioka, S. Nishikawa, S. Nakajima et al., "Non hot-spot PV module using solar cells with bypass diode function," in Proceedings of the 25th IEEE Photovoltaic Specialists Conference,pp. 1271–1274, IEEE, May 1996.

[44] Standards Australia, "Installation of photovoltaic PV arrays," AS/NZS 5033, 2005.

[45] K. Kim and P. T. Krein, "Reexamination of photovoltaic hot spotting to show inadequacy of the bypass diode," IEEE Journal of Photovoltaics, vol. 5, no. 5, pp. 1435–1441, 2015.

[46] W. Herrmann, W. Wiesner, and W. Vaassen, "Hot spot investiga-tions on PV modules-new concepts for a test standard and con-sequences for module design with respect to bypass diodes," in Proceedings of the 26th IEEE Photovoltaic Specialists Conference, pp. 1129–1132, IEEE, Anaheim, Calif, USA, September-October 1997.

[47] S. Silvestre, A. Boronat, and A. Chouder, "Study of bypass diodes configuration on PV modules," Applied Energy, vol. 86, no. 9, pp. 1632–1640, 2009.

[48] V. Quaschning and R. Hanitsch, "Numerical simulation of current-voltage characteristics of photovoltaic systems with shaded solar cells," Solar Energy, vol. 56, no. 6, pp. 513–520, 1996.

[49] H. Kawamura, K. Naka, N. Yonekura et al., "Simulation of I–V characteristics of a PV module with shaded PV cells," Solar Energy Materials and Solar Cells, vol. 75, no. 3-4, pp. 613–621, 2003.

[50] E. Bende, N. Dekker, and M. Jansen, "Performance and safety aspects of PV modules under partial shading: a simulation study," in Proceedings of the 29th European Photovoltaic Solar Energy Conference and Exhibition (EU PVSEC '14), September 2014.

[51] F. Fertig, S. Rein, M. Schubert, and W. Warta, "Impact of junction breakdown in multi-crystalline silicon solar cells on hot spot formation and module performance," Cell, vol. 40, article 80, 2011.

[52] Geisemeyer, F. Fertig, W. Warta, S. Rein, and M. C. Schubert, "Prediction of silicon PV module temperature for hot spots and worst case partial shading situations using spatially resolved lock-in thermography," Solar Energy Materials and Solar Cells, vol. 120, pp. 259–269, 2014.

[53] B. A. Alsayid, S. Y. Alsadi, J. S. Jallad, and M. H. Dradi, "Partial shading of pv system simulation with experimental results," Smart Grid and Renewable Energy, vol. 4, no. 6, pp. 429–435, 2013.

[54] S. Hamdi, D. Saigaa, and M. Drif, "Modeling and simulation of photovoltaic array with different interconnection configura-tions under partial shading conditions for fill factor

evaluation," in Proceedings of the International Renewable and Sustainable Energy Conference (IRSEC '14), pp. 25–31, IEEE, Ouarzazate, Morocco, October 2014.

[55] M. Abdulazeez and I. Iskender, "Simulation and experimental study of shading effect on series and parallel connected pho- tovoltaic PV modules," in Proceedings of the 7th International Conference on Electrical and Electronics Engineering (ELECO '11), pp. I28–I32, Bursa, Turkey, December 2011.

ANNEXURE

ANNEXURE 1 : PUBLISHED PAPER

Solar Photovoltaic String Under Partial Condition With Irradiance

Anjali Verma[1], Mohd Javed Khan[2], Saif Ahmad[3]
[1, 2] Dept of ECE
[1, 2, 3] Integral University, Lucknow, U.P.

Abstract- *Partial shadowing has a significant impact on a solar system. It is implicitly assumed that the maximum power of a partially shaded photovoltaic system constantly declines as the shading heaviness increases since photovoltaic systems work by using sun irradiance to produce electricity. The literature has suggested that this might not be the case, nevertheless. When a specific critical point is reached, the maximum power of a partially shaded solar system under a set design and partial shading pattern can be significantly less susceptible to shading heaviness. In this essay, the effect of partial shading is examined, as well as the crucial location that lowers shading heaviness. In this study, solar modules are connected in series to create a photovoltaic string. The study of the P-V characteristic curve under various numbers of shaded modules and shading heaviness implies that when the irradiance of the shaded modules reaches a specific critical point, the photovoltaic string becomes insusceptible to shading heaviness. Depending on how many shaded modules there are, the critical point may change. With regard to various solar string diameters and the number of shadowed modules in the photovoltaic string, the equation developed in this study helps to identify the critical point.*

Keywords- Photovoltaic system, shading, irradiance, maximum power.

I. INTRODUCTION

Conventional electrical power generation based on coal-fired power plants introduces carbon emissions which cause air pollution to be released into the Earth's atmosphere. To tackle this problem, renewable energy is employed as an alternative mode of electrical power generation. Among the renewable energy options, photovoltaic solar power is getting more and more popular nowadays due to its abundantly available and inexhaustible nature [1–5]. The non-involvement of mechanical or moving parts in a photovoltaic power system also makes it more preferable than other renewable energy options [6]. In 2016, around 75 GW of solar photovoltaic capacity was installed worldwide, which is almost a 50% growth from about 50 GW in 2015 [7,8]. The significant growth in photovoltaic power systems promotes the popularity of photovoltaic power system research among renewable energy researchers.

Photovoltaic modules or solar panels are the most fundamental components in a photovoltaic power system which is used to convert solar energy to electrical power [9–13]. When a module is connected to a piece of measurement equipment, P-V characteristics will be obtained as illustrated in Figure 1 [14]. The P-V characteristics demonstrate the electrical power delivered by the photovoltaic module at different voltages.

In the presence of the P-V characteristics, the maximum power of the photovoltaic module can be tracked. For instance, the marked point in Figure 1.3shows the highest point of the P-V characteristics, which represents the maximum power delivered by the photovoltaic module[15]. The maximum power of the photovoltaic module is always harvested from the photovoltaic module for electricity generation purposes [16]. Therefore, it is important to determine the P-V characteristics of a photovoltaic module so that the maximum power can be tracked and harvested from the photovoltaic module.

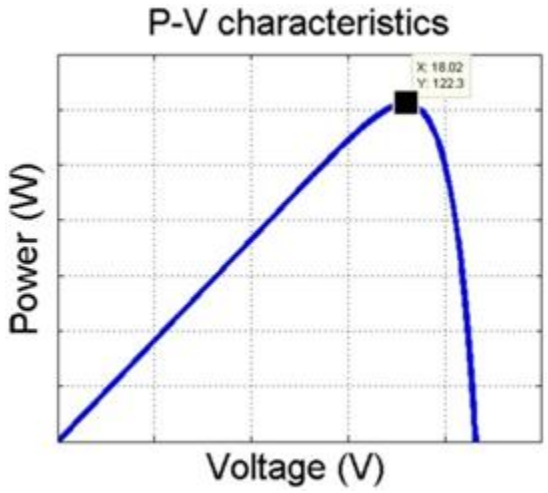

Figure 1. P-V characteristics of a photovoltaic module.

In a photovoltaic system, multiple photovoltaic modules are connected in series to form a photovoltaic string to achieve a required voltage and power output. To achieve an even higher power, these photovoltaic strings can be connected in parallel to form a photovoltaic array [17,18], as illustrated in Figure 2. In general, more than 1000 photovoltaic modules are employed in a megawatt-scale photovoltaic system to provide megawatts of electrical power production. These photovoltaic modules cannot only be connected in series as this will introduce an extremely high output voltage

which makes it unfit for grid-connected inverters and energy storage purposes. Therefore, parallel connection is employed, as well as series connection, to connect these photovoltaic modules. Usually, multiple photovoltaic strings are formed by connecting multiple photovoltaic modules in series. These photovoltaic strings are then connected in parallel to form the photovoltaic array in the megawatts scale photovoltaic plant. Similar to the photovoltaic module, the P-V characteristics of a photovoltaic string/array need to be determined in order to track and harvest the maximum power from the photovoltaic string/array.

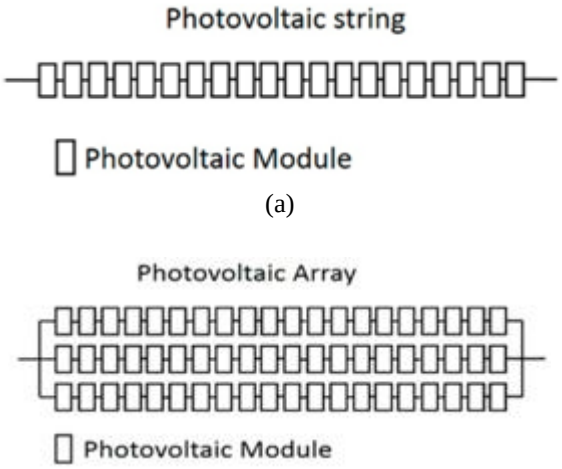

Figure 2. Photovoltaic system: (**a**) Photovoltaic string; (**b**) Photovoltaic array.

During a uniform irradiance condition, the P-V characteristics of a photovoltaic string exhibit one peak that resembles the P-V characteristics in Figure 1. The peak acts as the global peak which represents the maximum power of the photovoltaic string [19,20]. When partial shading takes place, multiple peaks appear on the P-V characteristics due to the use of a bypass diode [21–23]. Figure 3 shows the P-V characteristics of a photovoltaic string during a partial shading condition. The highest peak is the global peak which represents the maximum power of the photovoltaic string, while the others are the local peaks [24,25].

Apparently, a photovoltaic system is highly susceptible to partial shading [26–39]. During partial shading, the maximum power of a photovoltaic system can drop drastically, which significantly reduces the energy yield of the photovoltaic system. However, the susceptibility of partial shading to a photovoltaic system is not constant. The susceptibility of partial shading to a photovoltaic system can be varied due to the partial shading pattern and the connection employed to connect the photovoltaic modules in the photovoltaic system [26–29,32–38].

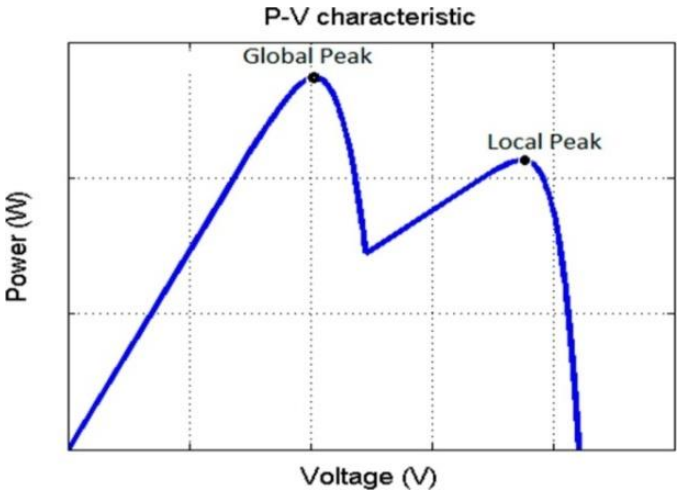

Figure 3. P-V characteristics of photovoltaic string under partial shading.

The experimental results in [26] suggested that under an identical partial shading pattern, the maximum power of a photovoltaic system should drop at a constant rate as the shading heaviness increases, as illustrated in Figure 1.6a. It means that under an identical partial shading pattern, a partially shaded photovoltaic system is always susceptible to the shading heaviness. This makes sense as the photovoltaic system relies on the solar irradiance to generate electrical power, and the maximum power of a partially shaded photovoltaic system should be lower and lower as the shading heaviness is getting heavier and heavier.

However, another phenomenon has been observed by S. Silvestre et al. [39]. S. Silvestre et al. discovered that a partially shaded photovoltaic system is not necessarily susceptible to the shading heaviness. They discovered that the maximum power of a partially shaded photovoltaic system decreases as the shading heaviness increases, as presented by the researchers in [26–38]. However, when the shading heaviness reaches a certain critical point, the maximum power remains unchanged even if the shading heaviness is getting heavier and heavier from that critical point, as illustrated in Figure 4 b. It means that the partially shaded photovoltaic system can become insusceptible to shading heaviness when the shading heaviness reaches a certain critical point. This finding is inspiring because a partially shaded photovoltaic system is commonly believed to always be susceptible to the shading heaviness.

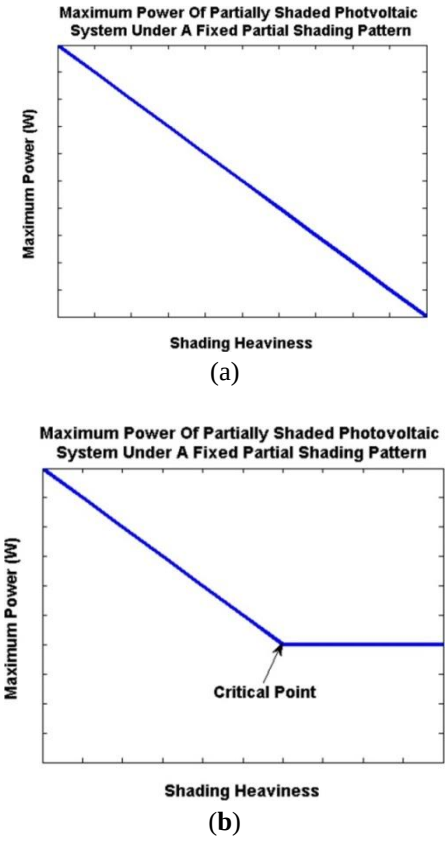

Figure 4. Maximum power of a partially shaded photovoltaic system under a fixed partial shading pattern

(**a**) as suggested by the experimental results in [26];
(b) as suggested by the experimental results in [39].

It is obvious that lots of research has been conducted on the impact of partial shading on the photovoltaic system throughout the years [26–38]. However, none of it has precisely presented the finding proposed in [39], which stated that the maximum power of a partially shaded photovoltaic system can become insusceptible to shading heaviness when the shading heaviness reaches a certain critical point. Therefore, it is a good area to further explore.

The finding proposed by [39] regarding the critical point is definitely inspiring. However, the experiment setup used in their research is a photovoltaic system that consists of nine photovoltaic modules only. They did not consider cases where a photovoltaic system consists of a greater number of photovoltaic modules. Besides that, the partial shading pattern and shading heaviness applied in their experiment are limited, which is insufficient to really conclude their finding. According to their result, the critical point can vary based on the number of shaded modules in the photovoltaic system. Therefore, an equation to determine the critical point for different numbers of shaded modules is highly expected. However, they did not formulate an equation to determine the critical point. Furthermore, they did not verify whether the critical point is also applicable to different sized photovoltaic systems.

The aim of this research is to investigate the susceptibility of the shading heaviness to a partially shaded photovoltaic system and the critical point that decreases the susceptibility of shading heaviness using a photovoltaic system with a multiple number of photovoltaic modules and various partial shading conditions. Besides that, an equation to calculate the critical point is formulated in this research as well. Furthermore, the critical point equation is also verified with different sized photovoltaic systems.

With the increasingly environmental problems and shortages of traditional fossil fuels, solar energy as clean and renewable energy has attracted more and more attention. Photovoltaic power generation which has advantages of simplicity and convenience can directly convert solar energy to electrical energy. Coupled with the advancement of technology, such as improving conversion efficiency of solar cells and reducing the cost of devices, photovoltaic power generation is used more widely and has developed many different forms, including grid-connected or utility-interactive PV systems and stand-alone photovoltaic systems. But some undesirable problems such as hot spot and islanding effect occur correspondingly.

Hot spot occurs if the characteristics of solar cells mismatch are shaded or faulty, which reduces the short current of the shaded cell. Once the operating current of module or system exceeds the short current of the affected cell, the cell is forced into reverse bias and starts to consume the power generated by unshaded cells, resulting in overheating[42]. When the temperature of the shaded cell rises highly enough, the encapsulant, like EVA, will melt and the back sheet, like TPT, will be broken down, even leading to fire [43]. In general, bypass diodes are adopted to inhibit the shaded cell to crack and reduce the formation of hot spot. And the necessary parameters of bypass diodes and the number of cells in a string protected by a diode are determined by the parameters of normal cells [44].The typical group size is approximately 12–24 cells per bypass diode. However, these principles neglect whether or not the maximum heating power of the shaded cell can meet the requirement. It is also shown that bypass diodes are effective at preventing hot spot in short PV string lengths but cannot satisfy the demands in typical panel string lengths [45].

II. METHODOLOGY

A photovoltaic string consists of 4 photovoltaic modules and is used to conduct the experiment in this research. The photovoltaic modules have an open circuit voltage of 21.6 V, short circuit current of 7.34 A ideality factor of 1.5, and series resistance of 0 ohm. Temperature, T = 25◦C is used for all the case studies in the experiment. Each photovoltaic module in the photovoltaic string has one bypass diode.

There are three experiment setups developed using the photovoltaic string, including 1 modules shaded, 2 modules shaded and 3 modules shaded setups.

Table 1 shows all the conditions that applied to every experimental setup. In the experiment, the P-V characteristics of every experimental setup under all the applied conditions are determined.

Table1. Conditions applied to the experimental setups.

Conditions	**Unshaded Modules Irradiance (W/m2)**	**Shaded Modules Irradiance (W/m2)**
1	1200	1000
2	1200	800
3	1200	600
4	1200	400
5	1200	200
6	1200	100

A photovoltaic array that consists of parallel connected photovoltaic strings and is not used in this research. This is because a photovoltaic system with a higher degree of parallelism is less susceptible to partial shading [32]. Similar statements are also suggested in [33–40], which address the fact that a higher degree of parallelism in a photovoltaic system can reduce the susceptibility of partial shading. Therefore, a photovoltaic array that consists of parallelism is not used in this research. Photovoltaic string that is in a series connected configuration is used in this research.

The random partial shading patterns with multiple shading heaviness are not used in this research. These partial shading patterns occur due to an uneven cloud distribution. It is more likely to be experienced by a megawatts scale photovoltaic plant. The area of the coverage of the photovoltaic string is not as big as a megawatts scale photovoltaic system. Therefore, the random partial shading patterns with multiple shading heaviness are not considered in this research.

There is not a standard rule for choosing the photovoltaic system size to conduct the partial shading experiment. The size can be chosen based on the designer and researcher preferences. For instance, Hiren Patel and Vivek Agarwal [26] chose photovoltaic arrays that consist of 300, 900, and 1000 photovoltaic modules; R. Ahmad et al. [29] chose photovoltaic arrays that consist of 20 and 25 photovoltaic modules; S. Silvestre et al. [39] chose a photovoltaic array consisting of nine photovoltaic modules, and so on. Regardless of the chosen size of the photovoltaic system, the experimental outcome should be applicable in certain ways to a megawatts scale photovoltaic plant as tacitly assumed among the researchers [26–39].

A photovoltaic string model is developed to carry out the experiment. A solar cell block from the Sim Electronics block set is used to develop the photovoltaic string model. This method of modelling has been used by J. C. Teo et al. to develop a photovoltaic string model [11]. They have conducted practical measurements to validate the photovoltaic string model in their research. Hence, it makes sense to use this method to develop the photovoltaic string model for the experiment.

The solar cell block is set to a five-parameter configuration m which is defined in Equations (1) and (2), where I is the output current, I_{PH} is the photo-generated current, I_O is the diode saturation current, V is the output voltage, R_S is the series resistance, N_S is the number of cells, V_T is the junction thermal voltage, A is the ideality factor, k is the Boltzman constant (1.3806503 × 10−23 J/K), T is the cell temperature, and q is the electron charge (1.6021765 × 10^{-19} C).

$$I = I_{PH} - I_0 exp\left(\frac{V+IR_S}{N_S V_T} - 1\right) \quad (1)$$

$$V_T = \frac{AKT}{q} \quad (2)$$

The short circuit current, open circuit voltage, series resistance, and ideality factor of the solar cell block are set according to the experiment requirements. To implement the bypass diode, the diode block from the Simscape block set is connected in antiparallel with the solar cell block, as shown in Figure 6.

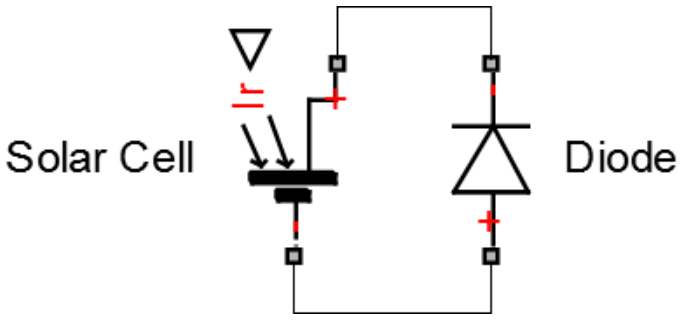

Figure 5. Solar cell block with bypass diode.

The architecture in Figure 5 represents a photovoltaic cell with a bypass diode. The architecture is duplicated to one sets, and these one sets of architecture are then connected in series to form a photovoltaic string model which consists of 4 photovoltaic modules that are required for the experiment. The photovoltaic string model is made into a single block known as PV string, as shown in Figure 6.

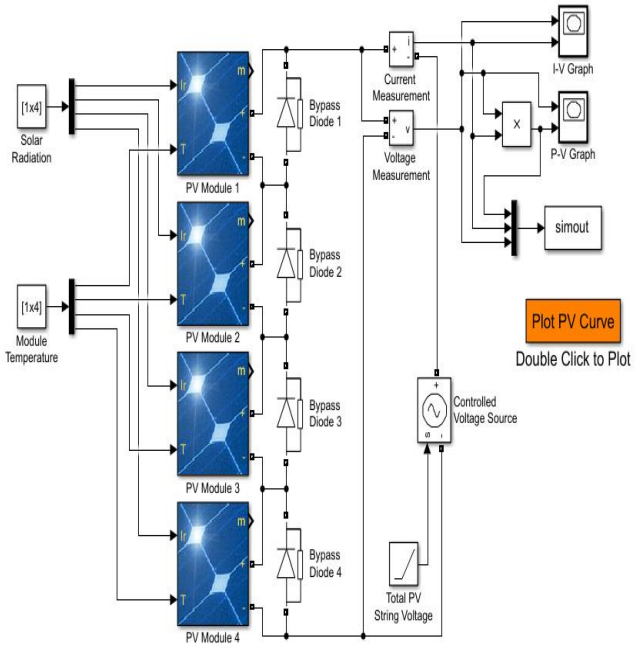

Figure 6. Photovoltaic string model.

Figure 6 shows the entire photovoltaic string model that was developed to carry out the experiment. The PV string block is the model for the photovoltaic string. It has 4 inputs which control the irradiance of every particular photovoltaic module in the photovoltaic string. The Control Unit block sets the unshaded modules irradiance, shaded modules irradiance, and number of the shaded modules in the PV string based on the parameter in the Unshaded Irr, Shaded Irr, and Shade Module block, respectively.

During the simulations, the Controlled Current Source block sweeps the output current of the photovoltaic string. The Voltage Sensor block measures the output voltage of the photovoltaic string. The Product block multiplies the output voltage and output current of the photovoltaic string to obtain the output power of the photovoltaic string. The To Workspace block sends the output power and output voltage of the photovoltaic string to the MATLAB (R2014a, MathWorks, Natick, MA, USA) workspace to plot the P-V characteristics curve.

Basically, the developed photovoltaic string model shown in Figure 6 is developed by cascading and extending the photovoltaic string model proposed by J. C. Teo et al. [11]. It is common practice to develop a larger scale photovoltaic system model by cascading and extending the validated small-scale photovoltaic system model [26]. The larger scale model that is developed by cascading and extending the validated small-scale model should give appropriate results for analysis purposes, as suggested by [26,39]. The method in [26] has also been applied by another researcher [29] to conduct a partial shading experiment.

The experiment can be conducted using the photovoltaic string model shown in Figure 3.2. To conduct the experiment for the three modules shaded setup, the Unshade Irr block is set to 1200 while the Shaded Module block is set to one. These settings configure the photovoltaic string to a three modules shaded setup with the unshaded modules irradiance fixed at 1200 W/m2. The Shade Irr block is set to 1000 to apply the condition 1 in Table 2 to the one modules shaded setup. Simulation performed under these setting generates the P-V characteristics of the one modules shaded setup under condition 1. To obtain the P-V characteristics of the one modules shaded setup under all the conditions in Table2, 6 simulations are performed with the Shade Irr block set to 100, 200, 400, , 600, 800 and 1000, respectively.

Similar procedures are applied to conduct the experiment for the two modules shaded, and three modules shaded setup. For instance, for the two modules shaded setup, the Unshade Irr block is set to 1200 while the Shade Module block is set to 1000 W/m2. These settings configure the photovoltaic string to the two modules shaded setup with the unshaded module irradiance fixed at 1000 W/m2. To obtain the P-V characteristics of the two modules shaded setup under all the conditions in Table3, 16simulations are performed with the Shade Irr block set to 100, 200, 400, , 600, 800 and 1000, respectively.

To conduct the experiment for the three modules shaded setup, the Unshade Irr block is set to 1200 while the Shade Modules block is set to 1000W/m2. The simulations are performed with the Shade Irr block set to 100, 200, 400, 600,

800 and 1000, respectively, to obtain the P-V characteristics of the three modules shaded setup under the Tables 3.2–3.4show the parameters set in the model in Figure 6 to conduct the experiment for the one modules shaded, two modules shaded and three modules shaded setups.

Table 2. Parameters set in the model shown in Figure 6 to conduct the experiment for the one modules shaded setup with Parameter Set in Shade Module Block=1

Condition Applied to the Experiment Setup	Parameter Set in Unshade Irr Block	Parameter Set in Shade Irr Block
Condition 1	1200	1000
Condition 2	1200	800
Condition 3	1200	600
Condition 4	1200	400
Condition 5	1200	200
Condition 6	1200	100

Table 3. Parameters set in the model shown in Figure 6 to conduct the experiment for the two modules shaded setup Parameter Set in Shade Module Block=2

Condition Applied to the Experiment Setup	Parameter Set in Unshade Irr Block	Parameter Set in Shade Irr Block
Condition 1	1200	1000
Condition 2	1200	800
Condition 3	1200	600
Condition 4	1200	400
Condition 5	1200	200
Condition 6	1200	100

Table 4. Parameters set in the model shown in Figure 6 to conduct the experiment for the three modules shaded setup with Parameter Set in Shade Module Block=3

Condition Applied to the Experiment Setup	Parameter Set in Unshade Irr Block	Parameter Set in Shade Irr Block
Condition 1	1200	1000
Condition 2	1200	800
Condition 3	1200	600
Condition 4	1200	400
Condition 5	1200	200
Condition 6	1200	100

The experiment considers lots of partial shading conditions, including lightly shaded, heavily shaded, a small number of modules shaded, a big number of modules shaded, and lots of shading heaviness conditions. These partial shading conditions pretty much cover all the possible partial shading conditions that might be experienced by a photovoltaic string at the site. Hence, the data collected in the experiment should be sufficient to conclude the critical points of a photovoltaic string, as well as to formulate the equation to determine the critical points of a photovoltaic string. However, more simulation work is required to conduct the experiment as it involves a huge number of partial shading conditions.

III. RESULT

Figure 7 shows the P-V characteristics of the one modules shaded setup. Figure 4.1a represents the P-V characteristics when the shaded modules irradiance is between 500 and 900 W/m2. Figure 4.1b illustrates the P-V characteristics when the shaded modules irradiance is between 0 and 400 W/m2. Considering the one modules shaded setup in Figure 7a, the higher voltage peak of the P-V characteristics is higher than the lower voltage peak when the shaded module irradiance is between 800 and 900 W/m2.

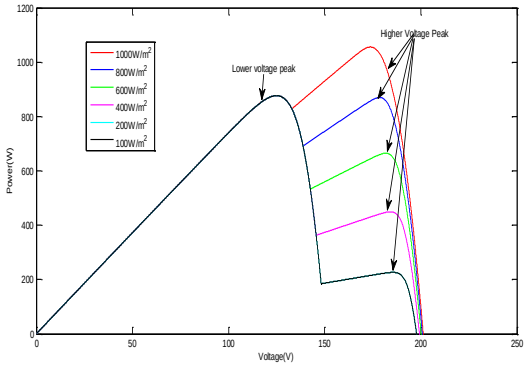

Figure 7. P-V characteristics of the one modules shaded setups: shaded modules irradiance is between 1000 and 100 W/m2;

Figure 8 shows the P-V characteristics of the two modules shaded setup. Figure 8a represents the P-V characteristics when the shaded modules irradiance is between 500 and 900 W/m2. Figure 8b illustrates the P-V characteristics when the shaded modules irradiance is between 0 and 400 W/m2. Similar situations are observed in the two modules shaded setup shown in Figure 8, where the higher voltage peak acts as the global peak when the shaded modules irradiance is above a certain level. The higher voltage peak reduces as the shaded modules irradiance decreases.

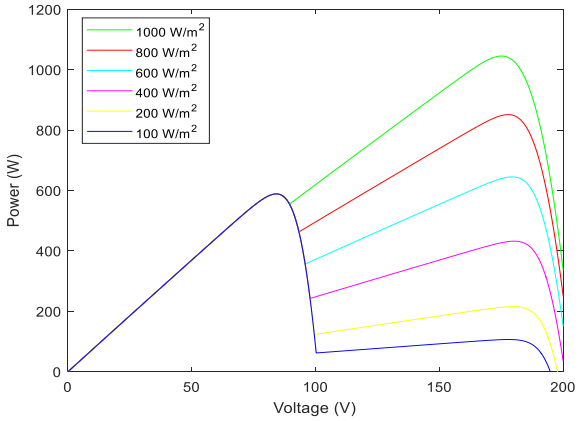

Figure 8. P-V characteristics of the two modules shaded setups: shaded modules irradiance is between 1000 and 100 W/m2;

Figure 9 shows the P-V characteristics of the three modules shaded setup. The similar situation that is observed in the one and two modules shaded setups is also observed in the three module shaded setups shown in Figures 9 . The higher voltage peak acts as the global peak when the shaded modules irradiance is above a certain level.

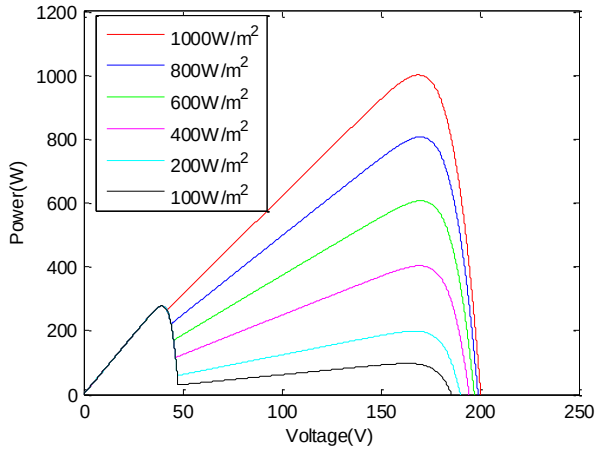

Figure 9. P-V characteristics of the three modules shaded setups: shaded modules irradiance is between 1000 and 100 W/m2

Tables 5– 8 are tabulated based on the data on the P-V characteristics of Figures 7–9 which show the maximum power and maximum power delivery voltage of all the experimental setups under the applied conditions.

Table 5. Maximum powers of the one modules shaded setup with Unshaded Module Irradiance (1000 W/m^2)

Unshaded Module Irradiance (W/m2)	**shaded Module Irradiance (W/m2)**	**Maximum Power (W)**	**Delivery Voltage (V)**
1200	1000	1055.8	174
1200	800	876.85	125
1200	600	876.84	125
1200	400	876.83	125
1200	200	876.82	125
1200	100	876.81	125

Table 6. Maximum powers of the two modules shaded setup with Unshaded Module Irradiance (1000 W/m^2)

Unshaded Module Irradiance (W/m2)	**shaded Module Irradiance (W/m2)**	**Maximum Power (W)**	**Delivery Voltage (V)**
1200	1000	1025.6	171
1200	800	835.695	173
1200	600	633.548	176
1200	400	577.055	82.13
1200	200	577.038	82.13
1200	100	577.029	82.13

Table 7. Maximum powers of the Three modules shaded setup with Unshaded Module Irradiance (1000 W/m^2)

Unshaded Module Irradiance (W/m2)	**shaded Module Irradiance (W/m2)**	**Maximum Power (W)**	**Delivery Voltage (V)**
1200	1000	1001.1	170.1
1200	800	806.898	170.2
1200	600	606.607	171.9
1200	400	403.088	171.8
1200	200	277.268	39.43
1200	100	277.255	39.43

By using the maximum powers and shaded modules irradiance in Table 5, a graph such as that illustrated in Figure 10 can be plotted. It shows the relationship between the maximum powers and the shaded modules irradiance of the one modules shaded setup.

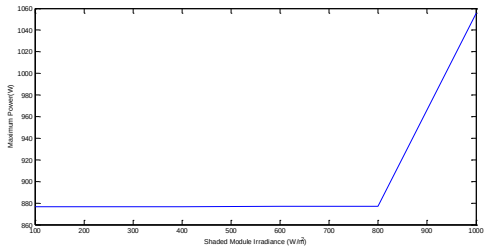

Figure 10. Maximum power versus shaded modules irradiance (one modules shaded).

Similar procedures are applied to Tables 6–7 to obtain the relationship between the maximum powers and the shaded modules irradiance for the 2 and 3 modules shaded setups. Figure 11 shows the relationship between the shaded modules irradiance and the maximum powers for all the experimental setups.

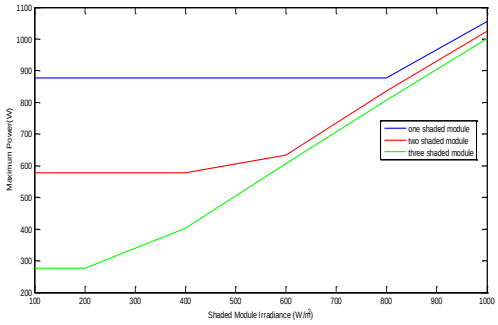

Figure 11. Maximum power versus shaded modules irradiance (all experiment setups).

V. CONCLUSION

Photovoltaic systems are highly susceptible to partial shading. The maximum power of a photovoltaic system can reduce drastically when partial shading takes place. The susceptibility of partial shading can vary based on the partial shading patterns, shading heaviness, and the configuration employed in connecting all the photovoltaic modules in the photovoltaic system. Under a fixed configuration and partial shading pattern, the maximum power of a partially shaded photovoltaic system is tacitly assumed to decrease at a constant rate as the shading heaviness increases. This tacit assumption is proposed based on the functionality of a photovoltaic system that relies on solar irradiance to generate electrical power. However, some researchers discovered that the maximum power under a fixed configuration and partial shading pattern can be highly insusceptible to shading heaviness when a certain critical point is met. Furthermore, the critical point can vary based on the number of shaded modules in a photovoltaic system. The novelty of this research includes the formulation of the equation to determine the critical point that is applicable to different photovoltaic system sizes and numbers of shaded modules in a photovoltaic system. Besides that, the equation has been verified with different sized photovoltaic systems as well. When 40% of photovoltaic modules in the photovoltaic system are shaded under an identical partial shading pattern, the maximum power drops by approximately 16.27% for every 100 W/m2 drop in the shaded module irradiance as the shaded modules irradiance lies between 1000 and 600 W/m2. However, when the shaded modules irradiance lies between 600 and 100 W/m2, the maximum power drops only by 9.07% for every 100 W/m2 drop in the shaded module irradiance..

REFERENCES

[1] K. J. R. Liu, A. K. Sadek,W. Su, and A. Kwasinski, Cooperative Communications and Networking. New York City, NY, USA: Cambridge University Press, 2009.

[2] P. N. Son and H. Y. Kong, “Cooperative communication with energy-harvesting relays under physical layer security,” IET Commun., vol. 9, no. 17, pp. 2131–2139, Nov. 2015.

[3] R. Fan, J. Cui, S. Jin, K. Yang, and J. An, “Optimal node placement and resource allocation for UAV relaying network,” IEEE Commun. Lett., vol. 22, no. 4, pp. 808–811, Apr. 2018.

[4] M. Ju and H.-C. Yang, “Optimum design of energy harvesting relay for two-way decode-and forward relay networks under max-min and max-sum criterions,” IEEE Trans. Commun., vol. 67, no. 10, pp. 6682–6697, Oct. 2019.

[5] K. Sultan, “Best relay selection schemes for NOMA based cognitive relay networks in underlay spectrum sharing,” IEEE Access, vol. 8, pp. 190 160–190 172, 2020.

[6] A. Sendonaris, E. Erkip, and B. Aazhang, “User cooperation diversity-part I: System description,”IEEE Trans. Commun., vol. 51, no. 11, pp. 1927–1938, Nov. 2003.

[7] “User cooperation diversity-part II: Implementation aspects and performance analysis,” IEEE Trans. Commun., vol. 51, no. 11, pp. 1939–1948, Nov. 2003.

[8] R. U. Nabar, H. Bolcskei, and F. W. Kneubuhler, “Fading relay channels: Performance limits and space-time signal design,” IEEE J. Sel. Areas Commun., vol. 22, no. 6, pp. 1099–1109, Aug. 2004.

[9] H. Cui, L. Song, and B. Jiao, “Multi-pair two-way amplify-and-forward relaying with very large number of relay antennas,” IEEE Trans. Wireless Commun., vol. 13, no. 5, pp. 2636–2645, May 2014.

[10] S. Luo and K. C. Teh, "Amplify-and-forward based two-way relay arq system with relay combination,"IEEE Commun. Lett., vol. 19, no. 2, pp. 299–302, Feb. 2015.

[11] D. Li, "Amplify-and-forward relay sharing for both primary and cognitive users," IEEE Trans. Veh.Technol., vol. 65, no. 4, pp. 2796–2801, Apr. 2016.

[12] Y. Dong, M. J. Hossain, and J. Cheng, "Performance of wireless powered amplify and forward relaying over Nakagami-mfading channels with nonlinear energy harvester," IEEE Commun. Lett.,vol. 20, no. 4, pp. 672–675, Apr. 2016.

[13] S. Li, K. Yang, M. Zhou, J. Wu, L. Song, Y. Li, and H. Li, "Full-duplex amplify-and-forward relaying: Power and location optimization," IEEE Trans. Veh. Technol., vol. 66, no. 9, pp. 8458– 8468, Sep. 2017.

[14] K. M. Rabie and B. Adebisi, "Enhanced amplify-and-forward relaying in non-Gaussian PLC networks,"IEEE Access, vol. 5, pp. 4087–4094, 2017.

[15] L. Jiang and H. Jafarkhani, "mmWave amplify-and-forward MIMO relay networks with hybrid precoding/combining design," IEEE Trans. Wireless Commun., vol. 19, no. 2, pp. 1333–1346, Feb. 2020.

[16] A. S. Ibrahim, A. K. Sadek, W. Su, and K. J. R. Liu, "Cooperative communications with relay selection:When to cooperate and whom to cooperate with?" IEEE Trans. Wireless Commun., vol. 7, no. 7, pp. 2814–2827, Jul. 2008.

[17] M. R. Bhatnagar, R. K. Mallik, and O. Tirkkonen, "Performance evalution of best-path selection in a multihop decode-and-forward cooperative system," IEEE Trans. Veh. Technol., vol. 65, no. 4, pp.2722–2728, Apr. 2016.

[18] Y. Gu and S. Aissa, "RF-based energy harvesting in decode-and-forward relaying systems: Ergodic and outage capacities," IEEE Trans. Wireless Commun., vol. 14, no. 11, pp. 6425–6434, Nov. 2015.

[19] G. T. Djordjevic, K. Kansanen, and A. M. Cvetkovic, "Outage performance of decode-and-forward cooperative networks over Nakagami-m fading with node blockage," IEEE Trans. Wireless Commun.,vol. 15, no. 9, pp. 5848–5860, Sep. 2016.

[20] H. Liu, Z. Ding, K. J. Kim, K. S. Kwak, and H. V. Poor, "Decode-and-forward relaying for cooperative NOMA systems with direct links," IEEE Trans. Wireless Commun., vol. 17, no. 12, pp.8077–8093, Dec. 2018.

[21] R. Fan, S. Atapattu, W. Chen, Y. Zhang, and J. Evans, "Throughput maximization for multihop decode-and-forward relay network with wireless energy harvesting," IEEE Access, vol. 6, pp.24 582–24 595, 2018.

[22] O. M. Kandelusy and S. M. H. Andargoli, "Outage performance of decode-and-forward (DF)-based multiuser spectrum sharing relay system with direct link in the presence of primary users' power,"IET Commun., vol. 12, no. 3, pp. 246–254, Feb. 2018.

[23] E. Li, X. Wang, Z. Wu, S. Hao, and Y. Dong, "Outage analysis of decode-and-forward two-way relay selection with different coding and decoding schemes," IEEE Syst. J., vol. 13, no. 1, pp.125–136, Mar. 2019.

[24] M. Asadpour, B. Van den Bergh, D. Giustiniano, K. A. Hummel, S. Pollin, and B. Plattner, "Micro aerial vehicle networks: an experimental analysis of challenges and opportunities," IEEE Commun.Mag., vol. 52, no. 7, pp. 141–149, Jul. 2014.

[25] K. Namuduri, S. Chaumette, J. H. Kim, and J. P. G. Sterbenz, UAV Networks and Communications. Cambridge University Press, 2017.

[26] K. P. Valavanis and G. J. Vachtsevanos, Handbook of Unmanned Aerial Vehicles. Springer, 2015.

[27] F. Ono, H. Ochiai, and R. Miura, "A wireless relay network based on unmanned aircraft system with rate optimization," IEEE Trans. Wireless Commun., vol. 15, no. 11, pp. 7699–7708, Nov. 2016.

[28] M. M. Azari, F. Rosas, K.-C. Chen, and S. Pollin, "Ultra reliable UAV communication using altitude and cooperation diversity," IEEE Trans. Commun., vol. 66, no. 1, pp. 330–344, Jan. 2018.

[29] M. M. Azari, F. Rosas, and P. Sofie, "Cellular connectivity for UAVs: Network modeling, performance analysis, and design guidelines," IEEE Trans. Wireless Commun., vol. 18, no. 7, pp.3366–3381, Jul. 2019.

[30] W. Wang, X. Li, M. Zhang, K. Cumannan, D. W. K. Ng, G. Zhang, J. Tang, and O. A. Dober, "Energy-constrained UAV-assisted secure communications with position optimization and cooperative jamming," IEEE Trans. Commun., vol. 68, no. 7, pp. 4476–4489, Jul. 2020.

[31] H. Shakhatreh, A. H. Sawalmeh, A. Al-Fuqaha, Z. Dou, E. Almaita, I. Khalil, N. S. Othman,A. Khreishah, and M. Guizani, "Unmanned aerial vehicles (UAVs): A survey on civil applications and key research challenges," IEEE Access, vol. 7, pp. 48 572–48 634, 2019.

[32] W. Ejaz, M. A. Azam, S. Saadat, F. Iqbal, and A. Hanan, "Unmanned aerial vehicle enabled IoT platform for disaster management," Energies, vol. 12, no. 14, p. 2706, Jul. 2019.

[33] Y. Zeng, R. Zhang, and T. J. Lim, "Wireless communications with unmanned aerial vehicles: opportunities and challenges," IEEE Commun. Mag., vol. 54, no. 5, pp. 36–42, May 2016.

[34] J. Zhao, F. Gao, Q. Wu, S. Jin, Y. Wu, and W. Jia, "Beam tracking for UAV mounted Sat Com on the-move with massive antenna array," IEEE J. Sel. Areas Commun., vol. 36, no. 2, pp. 363–375,Feb. 2018.

[35] Y. Zeng, R. Zhang, and T. J. Lim, "Throughput maximization for UAV-enabled mobile relaying

systems," IEEE Trans. Commun., vol. 64, no. 12, pp. 4983–4996, Dec. 2016.

[36] Y. Zhang, Z. Mou, F. Gao, L. Xing, J. Jiang, and Z. Han, "Hierarchical deep reinforcement learning for backscattering data collection with multiple UAVs," IEEE Internet Things J., vol. 8, no. 5, pp.3786–3800, Mar. 2021.

[37] J. Zhao, Y. Wang, Z. Fei, X. Wang, and Z. Miao, "NOMA-aided UAV data collection system: Trajectory optimization and communication design," IEEE Access, vol. 8, pp. 155 843–155 858,2020.

[38] F. Luo, C. Jiang, J. Du, J. Yuan, Y. Ren, S. Yu, and M. Guizani, "A distributed gateway selection algorithm for UAV networks," IEEE Trans. Emerg. Topics Comput., vol. 3, no. 1, Mar. 2015.

[39] R. Duan, J. Wang, C. Jiang, Y. Ren, and L. Hanzo, "The transmit-energy vs computation-delay trade-off in gateway-selection for heterogenous cloud aided multi-UAV systems," IEEE Trans.Commun., vol. 67, no. 4, pp. 3026–3039, Apr. 2019.

[40] M. Vaezi, R. Schober, Z. Ding, and H. V. Poor, "Non-orthogonal multiple access: Common myths and critical questions," IEEE Wireless Commun., vol. 26, no. 5, pp. 174–180, Oct. 2019.

[41] M. Vaezi and H. V. Poor, "NOMA: An information-theoretic perspective," in Multiple Access Techniques for 5G Wireless Networks and Beyond, M. Vaezi, Z. Ding, and H. V. Poor, Eds. Cham:Springer International Publishing, 2019, pp. 167–193.

[42] F. Mokhtari, M. R. Milli, F. Eslami, F. Ashtiani, B. Makki, M. Mirmohseni, M. Nasiri-Kenari, and T. Svensson, "Download elastic traffic rate optimization via NOMA protocols," IEEE Trans. Veh. Technol., vol. 68, no. 1, pp. 713–727, Jan. 2019.

[43] Z. Ding, M. Peng, and H. V. Poor, "Cooperative non-orthogonal multiple access in 5G systems,"IEEE Commun. Lett., vol. 19, no. 8, pp. 1462–1465, Aug. 2015.

[44] S. M. R. Islam, N. Avazov, O. A. Dobre, and K.-s. Kwak, "Power-domain non-orthogonal multiple access (NOMA) in 5G systems: Potentials and challenges," IEEE Commun. Surveys Tuts., vol. 19, no. 2, pp. 721–742, Second quarter 2017.

[45] 3GPP, "Study on network-assisted interference cancellation and suppression (NAICS) for LTE v.12.0.1," 3rd Generation Partnership Project (3GPP), Sophia Antipolis, France, Rep. TR 36.866, Mar. 2014.

[46] Media Tek, "Study on downlink multiuser superposition transmission (MUST) for LTE," 3rd Generation Partnership Project (3GPP), Hsinchu, Taiwan, Rep. TR 36.859, Apr. 2015.

[47] B. Wu, J. Chen, J. Wu, and M. Cardei, "A survey of attacks and countermeasures in mobile ad hoc networks," in Wireless Network Security, Y. Xiao, X. S. Shen, and D.-Z. Du, Eds. Boston, MA,USA: Springer, 2007, ch. 5, pp. 103–135.

[48] Y. Wang, G. Attebury, and B. Ramamurthy, "A survey of security issues in wireless sensor networks,"IEEE Commun. Surveys Tuts., vol. 8, no. 2, pp. 2–23, Second Quarter 2006.

[49] T. T. Karygiannis and L. Owens, "Wireless network security: 802.11, bluetooth and handheld devices," Gaithersburg, MD, USA, Nov. 2002.

[50] P. W. Shor, "Algorithms for quantum computation: discrete logarithms and factoring," in Proc.IEEE Annu. Symp. Found. of Comput. Sci. (FOCS), Santa Fe, NM, USA, Nov. 1994.

[51] R. K. Nichols and P. C. Lekkas, Wireless Security: Models, Threats, and Solutions. New York,NY, USA: McGraw-Hill, 2002.

[52] M. Bloch and J. Barros, Physical-Layer Security: From Information Theory to Security Engineering.Cambridge, United Kingdom: Cambridge University Press, 2011.

[53] A. D. Wyner, "The wire-tap channel," Bell Syst. Tech. J., vol. 54, no. 8, pp. 1355–1387, 1975.